Extracting Information from a Superradiant Burst Using Simple Measurements

Federico Belliardo,[1,*] Anjun Chu,[1] Martin Koppenhöfer,[2] and Aashish A. Clerk[1,†]
[1]Pritzker School of Molecular Engineering, University of Chicago, Chicago, Illinois 60637, USA
[2]Fraunhofer Institute for Applied Solid State Physics IAF, Tullastraße 72, 79108, Freiburg, Germany

(Received 31 March 2026; revised 4 August 2026; accepted 21 October 2026; published 12 November 2026)

It is well known that superradiant decay of an ensemble of N spins generates a complex non-classical state of light. Here, we consider the estimation of a phase encoded in the initial spin state from a superradiant burst of photons: how is information about this phase distributed among the emitted photons and can the phase be estimated using simple measurements? Despite the complexity of the photonic burst state, we show that a simple homodyne measurement combined with an optimized filter and linear estimator recovers the N-scaling of the quantum Fisher information of the initial spin state (including cases exhibiting N^2 Heisenberg scaling). Even more surprising, the temporal mode with optimal information content contains a vanishing fraction of the total emitted photons in the large-N limit, suggesting an effective compression of phase information. Our results and setup represent a new approach to quantum metrology for spin systems, in that they enable cavity-based readout of solid-state spin ensembles that utilizes resonant spin-photon interactions.

DOI: 10.1103/1m4s-kky2

I. INTRODUCTION

Dicke superradiance, the sudden and bright burst of radiation from an ensemble of N coherently emitting atoms, is perhaps the most paradigmatic example of a collective many-body phenomenon in quantum optics [1–3]. It has seen a recent resurgence of interest, spurred by new theoretical developments (see, e.g., Refs. [4–10]), as well as experiments (see, e.g., Refs. [11–16]). There is considerable interest in trying to understand and even harness the properties of the complex light field generated by this emission process. Recent work has studied how photons in the burst field are non-trivially distributed across multiple temporal modes [17–19], and how its non-classical properties could be used to drive an interferometer, enabling quantum-enhanced phase estimation [20–23].

From a quantum-metrology perspective, information in a spin ensemble is conventionally extracted either by a direct projective measurement of a spin observable or, for a continuously driven sensor, from a continuous measurement record of the environment [24,25]. In this work, we turn to another aspect of superradiant emission that has both fundamental and practical relevance: what is the *information content* of the superradiant burst of photons and can this information be extracted using simple linear measurements? We imagine the generic situation sketched in Fig. 1: a fully excited spin ensemble in a cavity has an infinitesimal parameter φ imprinted upon it (e.g., via a standard Ramsey protocol), before decaying superradiantly through the cavity into a waveguide. The initial information content of the spin ensemble (as quantified by the quantum Fisher information) must necessarily be transferred to the output N-photon waveguide state [26]. We ask how this information is distributed between the emitted photons and corresponding temporal modes, and whether a simple measurement can be used to extract it.

Our work provides a comprehensive study of how information in the initial spin state becomes encoded in the photons of the superradiant burst. It reveals several surprises. Despite the non-classical and inherently multimode nature of the superradiant emission burst, we show that one can extract almost half of the quantum Fisher information of the initial state using an extremely simple measurement protocol: a homodyne measurement that isolates a single temporal mode via an optimized filter, combined with a simple linear estimator. The resulting filtering problem is the finite-duration, nonstationary analogue of a generalized matched filter. In a scenario where the noise is stationary, the optimal frequency-domain filter weights each signal component by the inverse noise spectrum, whereas here the temporal correlations of the burst require the inverse time-domain fluctuation kernel [27–30]. This result remains true even for cases where the Fisher information exhibits Heisenberg

*Contact author: federico.belliardo@gmail.com
†Contact author: aaclerk@uchicago.edu

Published by the American Physical Society under the terms of the Creative Commons Attribution 4.0 International license. Further distribution of this work must maintain attribution to the author(s) and the published article's title, journal citation, and DOI.

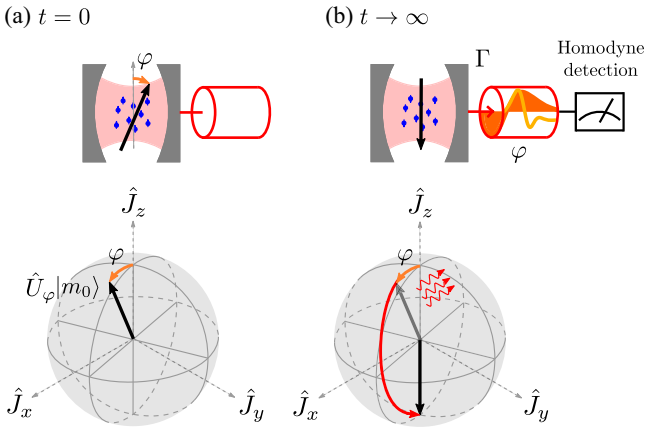


FIG. 1. (a) Generic setup and initial state: spin ensemble (with collective angular momentum operators $\hat{J}_\alpha$) in a cavity, where the spins have been infinitesimally perturbed from the fully excited state by a parameter-dependent unitary $\hat{U}_\varphi$. In the picture, the rotation angle $\varphi \simeq 0$ has been enhanced for clarity. This initial spin state has a quantum Fisher information $\mathcal{F}_\varphi$. (b) Long-time state: the spin ensemble decays superradiantly, with a φ-dependent photonic burst state generated in multiple temporal modes of the cavity's input-output waveguide. We show that for a variety of cases, a simple homodyne measurement that targets a single temporal mode of the output field can recover a constant fraction of $\mathcal{F}_\varphi$ in the large-N limit, even in cases where one has Heisenberg scaling.

scaling with the number of spins (via the so-called twist-untwist protocol [31,32]). Equally surprising, we find that the temporal mode with optimal information content is not the same as the mode that has the maximum number of photons. While for large N it is known that greater than 90% of emitted photons occupy a single temporal mode [19], we find that the temporal mode optimizing information in a homodyne measurement contains a vanishing fraction of the emitted photons: in the simplest case, the number of photons in this mode scales only as $\sim N^{2/3}$. If the encoding of the spin system happens through a Ramsey protocol, with no spin squeezing involved, we show that one can extract *all* of the information with time-resolved photon counting or homodyne measurement if one goes beyond a linear estimator and makes use of higher moments. We show this by making a connection between our setup and the problem of continuous metrology [25,33], and extending the recently derived results of Ref. [34].

Note that while the basic question we ask is of fundamental interest, it also has relevance to a variety of leading platforms that are being pursued for quantum metrology applications. There is growing interest in pursuing quantum metrology using solid-state spin ensembles (e.g., NV center defect spins in diamond) coupled to microwave or nanophotonic cavities, as well as studies of superradiance in such platforms (see, e.g., Refs. [35–37]). While the standard approach to cavity-based readout in such cases would be to use a non-resonant dispersive interaction [38], in some cases resonant approaches could be beneficial as they make use of the full cavity-spin coupling strength and hence could work considerably faster. Our analysis exactly describes such a resonant protocol where information is resonantly transferred from the spin ensemble to an outgoing photonic or microwave field via a superradiant decay. We also analyze cases where one uses a non-resonant spin-cavity interaction (still far from the dispersive regime) in order to slow down the superradiant burst; even in this case, we show that our basic approach is effective. A homodyne measurement using an optimal filter is still able to extract almost half of the initial state's quantum Fisher information, despite the increased complexity of the dynamics.

The rest of this manuscript is organized as follows. In Sec. II we introduce the physics of the superradiant ensemble of spins and our metrological spin-readout problem. In Sec. III we define temporal modes of the output field and apply homodyne detection to the estimation problem. In Sec. IV we derive the optimal temporal mode to measure in homodyne detection with a linear estimator (i.e., the mode that maximizes the signal-to-noise ratio) and discuss its properties. In Sec. V we discuss how our results change when including collective spin-spin interactions (arising from a non-zero spin-cavity detuning). Finally, in Sec. VI we discuss the achievability of the ultimate quantum limit going beyond the use of filters and linear estimators.

Note that our setting is distinct from works studying metrology with SR lasers [11,39–41], which focus on continuous estimation of the coherence of a pumped spin ensemble; in contrast, our goal is to read out information initially encoded in an ensemble without the use of any driving. Our setting, where we study the transient light emitted by the superradiant ensemble, is also very different from driven steady-state realizations of collective fluorescence or superradiance, where the emitted field probes a nonequilibrium steady state rather than a finite burst carrying information from an initially encoded spin state [11,42,43]. Our problem also has minimal overlap with other works studying superradiance for metrology, including non-classical input states for interferometers [18,20,21], readout using spin amplifiers [44,45], and readout using disordered superradiance [46].

II. MODEL AND GENERIC QUANTUM METROLOGY PROTOCOL WITH A SPIN-ENSEMBLE SENSOR

A. Basic model

We consider a generic setup (as sketched in Fig. 1) where an ensemble of N identical spin-1/2 systems acts as a sensor and is coupled to a single bosonic mode (a cavity or resonator mode) that will ultimately be used for readout. Working in a rotating frame set by the spin Larmor

frequency, the Hamiltonian of the system takes the form of a Tavis-Cummings model:

$$\hat{H} = \Delta \hat{a}^\dagger \hat{a} + g(\hat{J}_+ \hat{a} + \hat{J}_- \hat{a}^\dagger), \tag{1}$$

where Δ is the detuning between the cavity and the spins, and g is the strength of the collective coupling of the spins and the cavity. $\hat{a}$ is the cavity mode annihilation operator, while the spin ensemble is described by collective angular momentum raising and lowering operators, $\hat{J}_+$ and $\hat{J}_-$. We will use $|m\rangle$ to denote standard Dicke states, i.e., states with a maximum total angular momentum $j_{\text{tot}} = N/2$ and a $\hat{J}_z$ eigenvalue m. We focus throughout on fully collective dynamics that conserves the total angular momentum of the spin ensemble.

We write the evolution of the system in a frame of reference corotating with the spins, and we work in the standard regime where the coupling between the spins and the cavity is sufficiently weak compared to the loss of the cavity ("bad-cavity" regime), such that the cavity can be adiabatically eliminated [47]. In this limit, the density matrix $\hat{\rho}$ of the spin ensemble obeys a Lindblad-style master equation that has cavity-mediated collective interactions and collective decay:

$$\frac{\mathrm{d}\hat{\rho}(t)}{\mathrm{d}t} = -i[\chi \hat{J}_z^2, \hat{\rho}(t)] + \mathcal{D}[\sqrt{\Gamma}\hat{J}_-]\hat{\rho}(t), \tag{2}$$

with $\Gamma \equiv 4g^2\kappa/(4\Delta^2 + \kappa^2)$ and $\chi \equiv 4g^2\Delta/(4\Delta^2 + \kappa^2)$, and $\mathcal{D}[\sqrt{\Gamma}\hat{J}_-](\cdot) = \Gamma(\hat{J}_- \cdot \hat{J}_+ - \frac{1}{2}\{\hat{J}_+\hat{J}_-, \cdot\})$. The coherent term generated by eliminating a detuned cavity can equivalently be written in terms of $\hat{J}_+\hat{J}_-$: in the symmetric manifold, $\hat{J}_+\hat{J}_- = j_{\text{tot}}(j_{\text{tot}} + 1) - \hat{J}_z^2 + \hat{J}_z$. The constant term is irrelevant, and the linear $\hat{J}_z$ term is absorbed into the rotating frame, leaving the $\hat{J}_z^2$ interaction in Eq. (2). The collective bad-cavity condition is $Ng^2/[\Delta^2 + (\kappa/2)^2] \ll 1$ [48]. The time-scale of the superradiant burst is $t_{\text{SR}} \simeq \frac{\log N}{\Gamma(\Delta)N}$, which is independent of the detuning χ, as we discuss in detail in Sec. V, where we study the performance of our metrological strategy in the presence of detuning. Note that Eq. (2) has already been realized experimentally (see, e.g., Ref. [49]).

B. Encoding information in the initial spin state

The basic sensing protocol we study corresponds to a local parameter estimation problem and is depicted schematically in Fig. 1: a fully excited spin ensemble has an infinitesimal parameter φ encoded in it, after which it decays superradiantly, with information transferred to the photonic state (collected in a waveguide). Our goal is to understand how information on φ is distributed between the photons and temporal modes of the emitted photonic field, and whether it can be simply extracted using a linear homodyne measurement.

We start our analysis by discussing the first information-imprinting step in the protocol. We assume that the initial state of the spin ensemble $|\psi_\varphi\rangle$ is given by the action of an infinitesimal unitary $\hat{U}_\varphi$ acting on a fully excited product state $|m = m_0\rangle$ with $m_0 = N/2$:

$$|\psi_\varphi\rangle \equiv \hat{U}_\varphi |m_0\rangle, \quad \text{with} \quad \hat{U}_\varphi \equiv \mathrm{e}^{i\varphi\hat{G}}. \tag{3}$$

We restrict our attention to cases where the parameter generator $\hat{G}$ is also a collective spin operator (i.e., it commutes with $\hat{J}^2$), e.g., $\hat{G} = \hat{J}_y$. The information content of the initial spin state is quantified by the quantum Fisher information (QFI), given by

$$\mathcal{F}_\varphi(|\psi_\varphi\rangle) = 4(\langle m_0|\hat{G}^2|m_0\rangle - \langle m_0|\hat{G}|m_0\rangle^2). \tag{4}$$

The most celebrated result of quantum metrology is the possibility of achieving Heisenberg scaling [50], i.e., $\mathcal{F}_\varphi(|\psi_\varphi\rangle) \propto N^2$, by using an entangled state of N probes (e.g., spins), instead of $\mathcal{F}_\varphi(|\psi_\varphi\rangle) \propto N$, which is the standard quantum limit (SQL) and arises when a separable state is used with a collective generator, acting identically on every spin [50,51]. Note that when all emitted photons are collected and there are no unobserved loss channels, it necessarily follows that at long times (after the superradiant decay is over), the QFI of the photonic state will be identical to the QFI of the initial spin state. Equivalently, the Cramér-Rao bound associated with this QFI is identical for measurements on the encoded spin state and on the total emitted light, provided all emitted modes are included.

In what follows, we will focus on two specific, experimentally relevant choices for $\hat{G}$. The first corresponds to $\hat{U}_\varphi$ performing a rotation of the spin ensemble around the y-axis, i.e., $\hat{G} = \hat{J}_y$. In this scenario the encoded state is

$$|\psi_\varphi^S\rangle \equiv \hat{U}_\varphi |m_0\rangle, \quad \text{with} \quad \hat{U}_\varphi \equiv \mathrm{e}^{i\varphi\hat{J}_y}, \tag{5}$$

which is separable and has $\mathcal{F}_\varphi(|\psi_\varphi^S\rangle) = N$. We stress that the spin coherent state $|\psi_\varphi^S\rangle$ is exactly the kind of state generated by a standard Ramsey sensing protocol [52]; the only difference here is that a final rotation is performed so that the spin ensemble is almost perfectly polarized in the $+z$ direction.

The second special generator we consider originates from the celebrated twist-untwist strategy for Heisenberg-limited metrology [31,32,53,54]. This strategy makes use of squeezing and anti-squeezing and is known to allow one to reach Heisenberg scaling with simple (even imperfect) projective measurements of the spin ensemble. We show that it is also useful when combined with the superradiant readout strategy sketched in Fig. 1. The twist-untwist protocol makes use of a unitary squeezing operator $\hat{U}_s \equiv \mathrm{e}^{iQ\hat{J}_x^2/N}$ generated by a one-axis twisting Hamiltonian.

It involves three stages: (i) squeeze an initial product state, (ii) perform a φ-dependent rotation of the spin ensemble, e.g., via a Ramsey sequence, (iii) perform an anti-squeezing operation corresponding to the unitary $\hat{U}_s^\dagger$. The resulting φ-dependent state (upon suitable rotation) thus takes the form

$$|\psi_\varphi^E\rangle \equiv e^{i\varphi \hat{G}}|m_0\rangle, \quad \text{with} \quad \hat{G} = \hat{U}_s^\dagger \hat{J}_y \hat{U}_s. \tag{6}$$

This state has the same QFI as the entangled state $\hat{U}_s|m_0\rangle$ (with respect to a parameter generator $\hat{J}_y$). The exact expression for this QFI, together with the generator matrix element that controls the homodyne SNR, is given in Appendix A. In that appendix, we see that, as a function of the squeezing parameter Q, the signal-to-noise ratio (SNR) of a projective measurement of $\hat{J}_y$ (corresponding to a simple linear estimator) is maximized at $Q = Q_{\text{opt}} \equiv N \arctan[1/\sqrt{N-2}] = N \operatorname{arccot}\sqrt{N-2}$ [31]. For this same choice, the QFI approaches $(1-e^{-2})N^2/2$ at large N. For this choice of Q, both the SNR and QFI exhibit Heisenberg scaling with N (although with different prefactors, see Appendix A). As our homodyne strategy seeks to replicate the information available in a direct $\hat{J}_y$ measurement, we will also set $Q = Q_{\text{opt}}$ in our analysis.

III. PHOTONIC OUTPUT FIELD: TEMPORAL MODES AND HOMODYNE MEASUREMENT

We return to Fig. 1 and now discuss the readout aspect of our generic metrology protocol, where the superradiant decay of the spin ensembles creates a propagating photonic state (the superradiant burst) whose quantum state depends on the parameter φ that was originally encoded in the spin ensemble. Our goal is to understand the information content of these photons, and whether a simple linear homodyne measurement is sufficient to capture this information. To set the stage for this discussion, we review homodyne measurement in our setup, as well as the temporal mode description of the output field.

A. Input-output theory and homodyne measurement

The photonic output field in the cavity is described by the operator $\hat{b}_{\text{out}}(t)$, as determined by standard quantum-optical input-output theory [55,56]. As we are working in the regime where the cavity mode $\hat{a}$ has been adiabatically eliminated, the basic input-output equation for the setup in Eq. (2) takes the form:

$$\hat{b}_{\text{out}}(t) = -i\sqrt{\Gamma}\hat{J}_-(t) + \hat{b}_{\text{in}}(t). \tag{7}$$

Both input and output fields satisfy $[\hat{b}_\alpha(t), \hat{b}_\alpha^\dagger(t')] = \delta(t-t')$, with $\alpha = \text{out/in}$, and the input field is taken to be vacuum noise (there is no driving of the cavity), implying $\langle \hat{b}_{\text{in}}^\dagger(t)\hat{b}_{\text{in}}(t')\rangle = 0$. We denote the initial joint state of spins and input radiation by $|\Psi_\varphi\rangle \equiv |\psi_\varphi\rangle \otimes |\Omega\rangle$, where $|\Omega\rangle$ is the vacuum of the input field. Whenever expectation values of spin-only operators with respect to $|\Psi_\varphi\rangle$ are calculated, we omit the vacuum state $|\Omega\rangle$ and write only the spin state $|\psi_\varphi\rangle$.

At least some information on the parameter φ will be available in $\langle \hat{b}_{\text{out}}(t)\rangle$ for times $t > 0$. We thus define the *signal function* $\alpha_I(t)$ by the parametric derivative of this average value with respect to φ:

$$\alpha_I(t) \equiv \left.\frac{\partial \langle \Psi_\varphi | \hat{b}_{\text{out}}(t) | \Psi_\varphi\rangle}{\partial \varphi}\right|_{\varphi=0}. \tag{8}$$

Using the input-output relation in Eq. (7) one finds that the signal function is given by

$$\alpha_I(t) = -i\sqrt{\Gamma}\left.\frac{\partial \langle \hat{J}_-(t)\rangle_\varphi}{\partial \varphi}\right|_{\varphi=0} = \sqrt{\Gamma}\langle m_0|[\hat{J}_-(t), \hat{G}]|m_0\rangle. \tag{9}$$

This relation directly follows from the definition of the average and reflects the structure of Kubo linear-response susceptibility (i.e., how $\hat{J}_-$ responds to an initial perturbation involving $\hat{G}$). In Appendix B, we compute the signal $\alpha_I(t)$ at resonance, $\chi = 0$, for the superradiant decay described by Eq. (2).

One might expect that the full time-dependence of $\alpha_I(t)$ would have a strong sensitivity to the form of $\hat{G}$. Surprisingly, this is not the case. The dynamics in Eq. (2) has a weak $U(1)$ symmetry generated by $\hat{J}_z$ [57], which gives the Lindbladian a block-diagonal structure, greatly constraining dynamics. A consequence is that for any collective generator $\hat{G}$, we have (see Appendix C):

$$\alpha_I(t) = -\langle m_0|\hat{G}|m_0 - 1\rangle \cdot \sqrt{\Gamma}\langle m_0 - 1|\hat{J}_-(t)|m_0\rangle \tag{10}$$

$$\equiv \langle m_0|\hat{G}|m_0 - 1\rangle \cdot \tilde{\alpha}_I(t). \tag{11}$$

We see that the time dependence of the signal function has a "universal" dependence on time, in that its shape does not depend on the choice of generator. The generator only sets an overall scale via the prefactor. The role of $\hat{G}$ is to seed the initial coherence that carries the encoded parameter φ; the subsequent decay dynamics are independent of the encoding generator. Furthermore, the one-point output amplitude probes only the single-coherence sector connecting $|m_0\rangle$ and $|m_0 - 1\rangle$; all other coherences generated by $\hat{G}$ are orthogonal to this amplitude and therefore do not contribute to the linear signal.

This result continues to hold for the full collective dynamics described by Eq. (2) (which has collective decay as well as spin-spin interactions), and even holds if we do not adiabatically eliminate the cavity and work with the

cavity in Eq. (1), with collective spin-spin interactions whose Hamiltonian preserves $\hat{J}_z$.

The information in the average output field can be captured by a homodyne measurement, a simple and ubiquitous linear measurement that yields a current $I(t)$ that is proportional to one quadrature of the output field. Using a time-dependent homodyne angle $\theta(t)$, the homodyne current operator is

$$\hat{I}(t) \equiv e^{i\theta(t)}\hat{b}_{\text{out}}(t) + \text{H.c.} \tag{12}$$

If one takes $\theta(t) = -\arg \alpha_I(t)$, the average homodyne-current response is maximized, and $\partial_\varphi \langle \hat{I}(t)\rangle = 2|\alpha_I(t)|$. Homodyne measurements are standard in quantum optical setups (where they are realized using local oscillators, beam-splitters, and photocounting [58]), as well as in microwave circuit QED setups, where they can be directly implemented using an IQ mixer.

To analyze the information available from a homodyne measurement, we also need to understand the fluctuations of $\hat{I}(t)$. As we are always considering an infinitesimal parameter φ, we can calculate these fluctuations at $\varphi = 0$. Further, our main focus will be to use a simple linear estimator for φ, i.e., the estimate of φ will be proportional to the (optimally weighted) time-integrated homodyne current. See Appendix D for the definition of the estimator and its precision. The estimation error will then be determined by the signal-to-noise ratio (SNR), and we only need to understand the homodyne current fluctuations at the level of their auto-correlation function (evaluated at $\varphi = 0$):

$$S_{II}(t', t) \equiv \langle \hat{I}(t')\hat{I}(t)\rangle - \langle \hat{I}(t')\rangle\langle \hat{I}(t)\rangle. \tag{13}$$

B. Temporal modes

Our goal will be to find an optimal filter for the homodyne current that maximizes the resulting SNR. This filtering naturally corresponds to a temporal mode decomposition of the output field. We briefly review this notion here. We introduce a mode function $u(t)$ (chosen to have unit $L_2[0, \infty)$ norm), and an associated bosonic operator

$$\hat{b}_u \equiv \int_0^\infty u(t)\hat{b}_{\text{out}}(t)\mathrm{d}t. \tag{14}$$

This is a canonical bosonic annihilation operator satisfying $[\hat{b}_u, \hat{b}_u^\dagger] = 1$; it corresponds to removing photons from the chosen temporal mode. By picking a set of mode functions that form a complete orthogonal basis, we can describe the output field using a set of commuting temporal mode operators $\{\hat{b}_{u_j}\}_{j=1}^\infty$. This gives a decomposition of the output field in a discrete basis of wavepackets [55].

There is a long history of analyzing the output field produced by superradiant decay in terms of temporal modes and their correlations (see, e.g., [19,59]). The standard focus has been to find an orthogonal mode basis where there are no first-order coherences between the modes. This corresponds to diagonalizing the $g_1(t, t')$ correlation matrix:

$$g_1(t', t) \equiv \Gamma\langle m_0|\hat{J}_+(t')\hat{J}_-(t)|m_0\rangle. \tag{15}$$

Given some mode $u(t)$, the most basic question is the computation of its average photon number $\bar{n}_u$:

$$\bar{n}_u \equiv \langle \hat{b}_u^\dagger \hat{b}_u\rangle = \int_0^\infty \mathrm{d}t'\mathrm{d}t\, u^*(t')g_1(t', t)u(t). \tag{16}$$

Of particular interest is the temporal mode $w_{\text{pop}}(t)$ that has a maximum average photon number:

$$w_{\text{pop}}(t) \equiv \underset{u(t)}{\text{argmax}} \int_0^\infty \mathrm{d}t'\mathrm{d}t\, u^*(t')g_1(t', t)u(t). \tag{17}$$

This mode is the eigenvector of $g_1(t', t)$ with the largest eigenvalue. The photon number distribution between temporal modes has been extensively studied in the case of pure superradiant decay, i.e., the resonant-cavity limit of Eq. (2) where $\chi = 0$ and there is only collective decay. As discussed in Ref. [19], the radiation emitted in superradiance is multimodal, but for large N, the most populated mode carries ∼90% of the photons, and the fraction of the photons carried by the other orthogonal modes decreases rapidly with the index of the mode. In Fig. 2 we plot $w_{\text{pop}}(t)$ for a superradiant ensemble of spins with $N = 512$. The SNRs reported in the figure for $w_{\text{pop}}(t)$ and $w_{\text{sig}}(t)$ are obtained by substituting the mode functions defined in Eqs. (17) and (21), respectively, into the general SNR expression in Eq. (22).

C. Linear estimators based on photon counting have no information

While the total average number of photons emitted in the superradiant process is fixed, $\bar{n}_{\text{tot}} = N$, the distribution of photons across different modes changes with the initial state. One might therefore expect photon counting in a selected mode to provide a useful linear estimator for φ. In Appendix E, we show that this is not the case for a fully excited initial state: for any Hermitian collective generator $\hat{G}$, the leading change in the mode photon number is $\mathcal{O}(\varphi^2)$, so its linear sensitivity vanishes. It follows that the total photon number sensitivity, being the sum of the sensitivities from all the modes, is also quadratic in the parameter. This result follows from the $U(1)$ symmetry of the dynamics and the initial state $|m_0\rangle = |j\rangle$. This analysis does not rule out the possibility that the noise is also vanishing, so that the SNR of the measurement is finite.

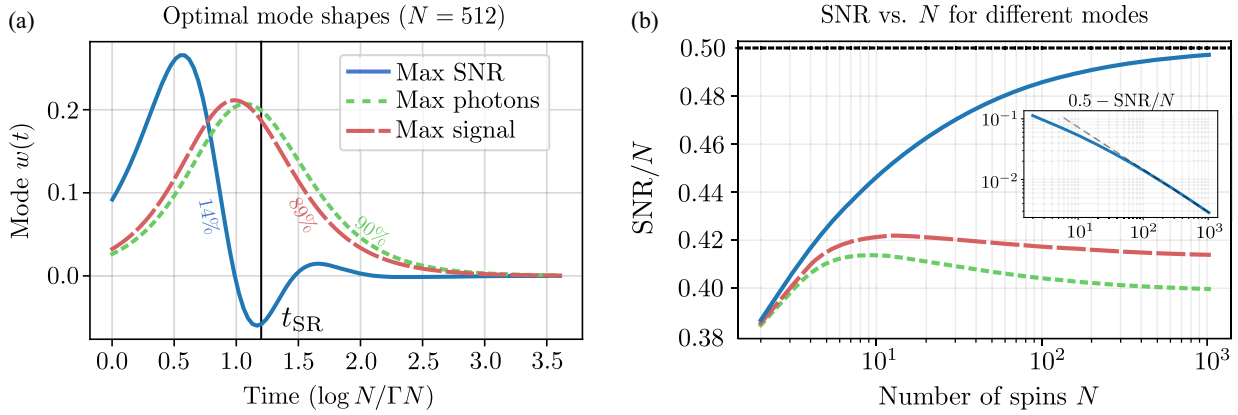


FIG. 2. (a) Mode profiles $w(t)$ for the maximum-photon mode [Eq. (17)], the maximum-signal mode [Eq. (21)] and the maximum-SNR mode [Eq. (26)]. Results are shown for pure superradiant decay dynamics [i.e., $\chi = 0$ in Eq. (2)], in which case these modes are real and independent of the generator $\hat{G}$ (up to an overall time-independent phase). We take $N = 512$. Each curve is labeled by the fractional photon number occupation of each mode $\bar{p}_u = \bar{n}_u/N$; for the maximum-SNR mode this ratio vanishes in the large-N limit. The vertical line indicates $t = t_{SR} \simeq \frac{\log N}{\Gamma N}$, the time associated with the peak intensity of the superradiant burst. (b) For a simple Ramsey encoding of a rotation angle, as described in Eq. (5), we evaluate the ratio of the SNR to the quantum Fisher information (which has the value N) as a function of N. For each mode shape this ratio converges to a constant as $N \to \infty$; in particular, for the maximum-SNR mode [Eq. (26)], the ratio converges to 0.5. The inset shows convergence to this value as a power law, $\frac{1}{2} - \frac{SNR}{N} \simeq 0.30 \cdot N^{-0.66}$. The line styles and colors label the three modes in the same manner as in panel (a). The maximum-photon and maximum-signal modes converge to an SNR lower than the SNR of $w_{SNR}(t)$, as expected.

Nevertheless, a zero-signal-over-zero-noise measurement strategy is considered impractical in an experimental context. This motivates homodyne detection as a practical linear readout strategy for the initial-value problem. In Appendix K we compute the classical Fisher information of time-resolved photon counting, which achieves the QFI in the resonant case, but this measurement is harder to realize than integrating the current of the homodyne measurement.

IV. MAIN RESULTS: INFORMATION CONTENT OF AN OPTIMAL HOMODYNE MEASUREMENT

Having established the basic description of our system, the sensing protocol, and the photonic output field, we now turn to our central question: *how much information on φ can be extracted from an optimized homodyne measurement?* We further restrict attention to the simplest and most experimentally friendly scenario, where the estimator for φ is proportional to some weighted time integral of the measured homodyne current. The question then becomes one of filtering: how do we filter the homodyne current to optimize the SNR of the measurement? This is equivalent to finding the optimal temporal mode $u(t)$ whose associated integrated homodyne current maximizes the SNR. A natural guess is that, since photons carry information on φ, more photons should yield better performance; hence, one should use the same temporal mode that maximizes the average photon number, cf. Eq. (17). Surprisingly, we now show that this guess is incorrect. In this section, we focus on the case of a resonant cavity, where $\chi = 0$ in the dynamics described by Eq. (2) (i.e., there is just collective superradiant decay, and no additional Hamiltonian spin-spin interactions). We address the impact of such interactions in the next section.

A. Optimal modes for maximum signal and maximum SNR

We first define the filtered homodyne current for a specific temporal mode $u(t)$ to be

$$\hat{I}_u(t) \equiv u(t)\hat{b}_{out}(t) + \text{H.c.}, \tag{18}$$

where the homodyne phase (i.e., local-oscillator phase) $\theta(t)$ has been absorbed into the definition of the complex mode function $u(t)$. Given a choice of mode function, the measured quantity will be the integrated and filtered homodyne current

$$\hat{M}_u \equiv \int_0^\infty dt\, \hat{I}_u(t). \tag{19}$$

Our estimate of φ will be proportional to the measured value of $\hat{M}_u$; hence, we define the net signal associated with this mode to be

$$\bar{S}_u \equiv \partial_\varphi \langle \hat{M}_u \rangle = 2\text{Re} \int_0^\infty dt\, u(t)\alpha_I(t). \tag{20}$$

We can now easily identify the temporal mode that maximizes the net signal $\bar{S}_u$. Denoting this mode as $w_{sig}(t)$,

we have:

$$w_{\rm sig}(t) \equiv \underset{u(t)}{\rm argmax}\, 2{\rm Re}\int_0^\infty {\rm d}t\, u(t)\alpha_I(t) = \frac{\alpha_I^*(t)}{\sqrt{\int_0^\infty {\rm d}\tau |\alpha_I(\tau)|^2}}. \tag{21}$$

Not surprisingly, the maximum-signal mode has the same shape and conjugate phase as $\alpha_I(t)$, and the mode-optimized value of the signal $\bar{S}_u$ is twice the L_2-norm of $\alpha_I(t)$.

While identifying the maximum-signal mode is straightforward and perhaps somewhat obvious, our goal is more involved: we want the mode $u(t)$ that optimizes the signal-to-noise ratio associated with a measurement of $\hat{M}_u$. For a given mode function $u(t)$, the power SNR is defined as

$${\rm SNR}[u(t)] \equiv \frac{|\bar{S}_u|^2}{\langle(\hat{M}_u - \langle\hat{M}_u\rangle)^2\rangle}, \tag{22}$$

where both the denominator and numerator are evaluated at $\varphi = 0$. The numerator is the square of the signal, while the denominator is the variance of the observable, i.e., ${\rm Var}(\hat{M}_u)$.

In Appendix G, we show how the fluctuations of the observable $\hat{M}_u$ can be computed from the correlation function for the filtered current, i.e.,

$$S_{II,u}(t',t) \equiv \langle\hat{I}_u(t')\hat{I}_u(t)\rangle - \langle\hat{I}_u(t')\rangle\langle\hat{I}_u(t)\rangle \tag{23}$$

defined in direct analogy with Eq. (13). The $U(1)$ weak symmetry of our dynamics under $\hat{J}_z$ rotations implies that there are no squeezing correlations in the output field. Using these symmetries and Eq. (7), we can introduce the fluctuation matrix

$$F(t',t) \equiv 2\Gamma\langle m_0|\hat{J}_+(t')\hat{J}_-(t)|m_0\rangle + \delta(t'-t). \tag{24}$$

As above, the spin-only expectation value is shorthand for the expectation value in $|\Psi_0\rangle = |m_0\rangle \otimes |\Omega\rangle$. The first term represents the contribution of the spin dynamics to the homodyne noise, whereas the second term is the usual shot-noise floor (stemming from vacuum fluctuations).

We can now define the temporal mode that maximizes the SNR, $w_{\rm SNR}(t)$, as

$$w_{\rm SNR}(t) \equiv \underset{u(t)}{\rm argmax}\, \frac{4|{\rm Re}\int_0^\infty {\rm d}t\; u(t)\alpha_I(t)|^2}{\int_0^\infty {\rm d}t' \int_0^\infty {\rm d}t\; u^*(t)F(t,t')u(t')}. \tag{25}$$

In Appendix G, we perform the optimization analytically and find

$$w_{\rm SNR}(t) = \frac{\int_0^\infty {\rm d}t'\, F^{-1}(t,t')\alpha_I^*(t')}{\sqrt{\int_0^\infty {\rm d}t \int_0^\infty {\rm d}t'\, \alpha_I(t)F^{-2}(t,t')\alpha_I^*(t')}}. \tag{26}$$

Note crucially that the maximum SNR mode $w_{\rm SNR}(t)$ is in general not identical to the maximum-signal mode $w_{\rm sig}(t)$. A special case is when the homodyne noise is white noise, i.e., $F(t,t') \propto \delta(t-t')$. For the more general case of temporally correlated noise, the maximum-SNR mode will be a tradeoff between optimizing the integrated signal and minimizing noise by making use of correlations [60].

For our superradiant decay dynamics, we have an even more striking result. By using the factorized expression for $\alpha_I(t)$ given in Eq. (11), we see that the form of the maximum-SNR mode $w_{\rm SNR}(t)$ is universal, i.e., it is independent of the specific form of the parameter generator $\hat{G}$ (up to an overall constant phase factor). We stress that while our derivation is fully quantum mechanical, the final result in Eq. (26) matches a well-known result in classical signal processing: it corresponds to the optimal "generalized matched filter" for extracting a signal waveform from a background of Gaussian noise (see, e.g., [27–30]). In a stationary-noise limit, this filter would weight each frequency component by the inverse noise spectrum; for a finite superradiant burst, the analogous operation is the time-domain kernel $F^{-1}(t,t')$.

We also stress another nice feature of our optimal-mode result: for the resonant cavity setup [cf. Eq. (2)], one finds that $\alpha_I(t)e^{-i\nu}$ is real at all times, where ν is a time-independent phase determined by the choice of generator $\hat{G}$ [i.e., $\nu = \arg\langle m_0|\hat{G}|m_0 - 1\rangle$, cf. Eq. (11)]. As a result, the phase of the maximum SNR mode is constant (modulo π) for all times. This yields a significant experimental simplification: the optimal information mode involves measuring the *same* output field quadrature at all times and does not require time-dependent control of the local-oscillator phase $\theta(t)$ in Eq. (12).

Using our knowledge of the maximum-SNR mode, we can also directly compute the optimized value of the SNR, i.e., the maximum SNR possible with a linear estimator obtained from the integrated homodyne measurement of a single mode. We find:

$${\rm SNR}[w_{\rm SNR}(t)] = 4\int_0^\infty {\rm d}t \int_0^\infty {\rm d}t'\, \alpha_I(t)F^{-1}(t,t')\alpha_I^*(t') \tag{27}$$

$$= |\langle m_0|\hat{G}|m_0 - 1\rangle|^2 \times 4\int_0^\infty {\rm d}t \int_0^\infty {\rm d}t'\, \tilde{\alpha}_I(t)F^{-1}(t,t')\tilde{\alpha}_I^*(t'). \tag{28}$$

Figure 2 shows plots of the three different "optimized" modes we have discussed here (optimized either for

maximum photon number, maximum net signal, or maximum SNR), for a large value of N. Several points are in order. First, note that the maximum-signal and maximum-photon modes have a similar shape: they exhibit no nodes and have a single peak at a time close to the time associated with the superradiant burst. While the mode shapes are similar, they are not identical. Second, and more importantly, the maximum-SNR mode has a shape *completely different* from the max-photon number mode. It changes sign and has a node slightly before the time of the superradiant burst. This sign change is a direct consequence of temporally correlated photonic noise produced by the superradiant burst: the maximum SNR mode is creating destructive interference from these correlations by having its sign change. Thus, the comparable resonant-case performance of $w_{\rm sig}$ and $w_{\rm SNR}$ shows that the two modes balance signal and correlated noise in different ways. Measuring $w_{\rm sig}$ is close to a classical strategy that keeps the largest mean response, whereas measuring $w_{\rm SNR}$ deliberately sacrifices part of this mean response so that different temporal portions of the output amplitude interfere destructively in the measured quadrature. The resulting noise cancellation is a property of the quantum temporal correlations generated by the superradiant decay, and it is also what allows the optimal mode to contain only a vanishing fraction of the emitted photons. In Appendix J, we compute explicitly the Fisher information of the homodyne measurement on the optimal mode and quantum Fisher information of the quantum state of the maximum SNR mode, and we show that these quantities are only slightly above the SNR of the linear measurement reported in this plot.

While it was suggested numerically in Ref. [19] that the asymptotic shape of the max-photon mode (and all other eigenfunctions of $g_1(t',t)$ defining a canonical orthonormal basis) converges in the large-N limit when the time is appropriately rescaled to the superradiant-burst timescale, we find no evidence for such convergence for the SNR-maximizing mode (see Fig. 3). This is consistent with the fact that the number of photons in the optimal mode scales sublinearly with N. If an asymptotic shape existed, there would be a stable asymptotic decomposition onto the eigenfunctions of $g_1(t',t)$, implying an asymptotic value for the fractional occupation number, which contradicts the scaling law found in Fig. 2. Since the number of photons in the higher-order modes of the canonical basis decreases exponentially fast with the mode index, while the fractional occupation number only scales as a power law in N, these higher-order modes, with an increasing number of nodes each, emerge very slowly in $w_{\rm SNR}(t)$ as N increases. This explains the slowly varying shape of the modes in Fig. 3. The most striking observation from this picture is that while the main maximum of the modes seems to have converged, the first negative lobe and the second positive lobe do not seem to be converging, indicating that they might be controlled by a timescale different from the one that controls the burst.

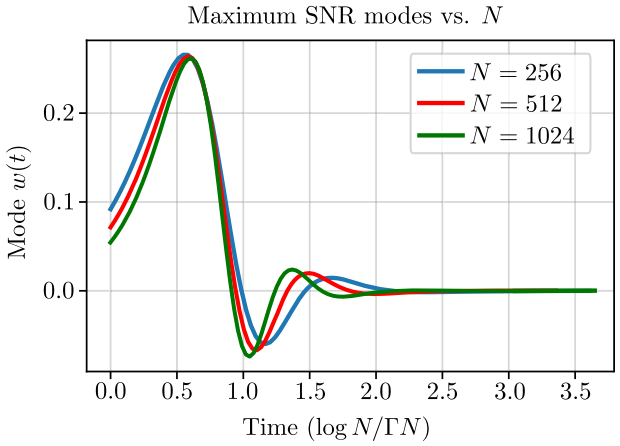


FIG. 3. Temporal modes maximizing the SNR, as computed in Eq. (26), for different values of the spin number N. We do not see any sign of convergence for the shape of the modes, when rescaled by the timescale of the superradiant burst.

We stress that the expressions in Eqs. (17), (21), and (25) can be used to analyze the information content of a homodyne measurement of a photonic field produced by arbitrary dynamics, as long as the output light has no squeezing correlations. When squeezing is present, one must instead use the generalized optimization derived in Appendix G.

B. Optimal homodyne measurement with a linear estimator allows Heisenberg-limited scaling

We are now in a position to state the main key result of our paper (again focusing initially on the resonant-cavity, $\chi = 0$ case): once we optimize the choice of mode (i.e., filter function), a simple homodyne measurement with a linear estimator achieves the same error scaling with N as the QFI of the original spin state $|\psi_\varphi\rangle$ at $t = 0$. Further, in the large-N limit, the optimized homodyne SNR converges to half the SNR of an idealized projective measurement of $\hat{J}_\alpha$ on the initial spin state. This is true for both an initial state corresponding to a simple Ramsey measurement (in which case we obtain SQL scaling, $\Delta\varphi \sim 1/\sqrt{N}$) and an initial state produced by an optimal twist-untwist spin-squeezing protocol (in which case we obtain HL scaling, $\Delta\varphi \sim 1/N$).

We can state these results more precisely by combining the exact generator-dependent factors in Appendix A with a numerical large-N evaluation of the universal fluctuation integral in Eq. (28) in the limit $N \to \infty$, for which we have

$$\int_0^\infty {\rm d}t \int_0^\infty {\rm d}t'\, \tilde{\alpha}_I(t) F^{-1}(t,t') \tilde{\alpha}_I^*(t') \to \frac{1}{2}, \qquad (29)$$

in the resonant scenario $\chi = 0$. For the case of an initial state produced by a Ramsey sequence [i.e., a parameter generator $\hat{G} = \hat{J}_y$, cf. Eq. (5)], we find:

$$\mathrm{SNR}[w_{\mathrm{SNR}}(t)] \sim \frac{N}{2} = \frac{1}{2}\mathcal{F}_{\varphi}(|\psi_{\varphi}^{S}\rangle) = \frac{1}{2}\mathrm{SNR}(|\psi_{\varphi}^{S}\rangle; \hat{J}_x) \quad \text{for } N \to \infty. \tag{30}$$

In contrast, for an initial state produced by an optimal twist-untwist sequence [cf. Eq. (6)], we obtain:

$$\mathrm{SNR}[w_{\mathrm{SNR}}(t)] \sim \frac{1}{2e}N^2 = \frac{1}{e(1-\mathrm{e}^{-2})} \times \mathcal{F}_{\varphi}(|\psi_{\varphi}^{E}\rangle) = \frac{1}{2}\mathrm{SNR}(|\psi_{\varphi}^{E}\rangle; \hat{J}_y) \quad \text{for } N \to \infty. \tag{31}$$

Here, $\mathrm{SNR}(|\psi_{\varphi}^{S}\rangle; \hat{J}_x)$ and $\mathrm{SNR}(|\psi_{\varphi}^{E}\rangle; \hat{J}_y)$ denote the SNRs of ideal projective measurements of the corresponding initial spin states; see Appendix A. Table 1 summarizes the asymptotic SNRs of ideal spin measurements and optimized homodyne measurements for both encoding protocols. We show the asymptotic convergence of the optimal mode SNR for the Ramsey encoding to its limiting value in Fig. 2. Note that if one instead performs a homodyne measurement using the maximum-photon mode $w_{\mathrm{pop}}(t)$ [cf. Eq. (17)], one obtains the same scaling behavior in N, with a slightly worse prefactor (see Fig. 2 again). The same is true if one uses the maximum-signal mode $w_{\mathrm{sig}}(t)$ [cf. Eq. (21)]. However, these conclusions change dramatically if one now considers the case where the cavity is detuned from the spin ensemble (something that might be necessary to slow down the superradiant decay to a reasonable timescale). As we discuss in the next section, the differences in the SNR for the maximum-SNR mode and the maximum-photon mode become much larger in this case. The only numerically evaluated ingredient in Eqs. (30) and (31) is the universal fluctuation-dependent integral in Eq. (28). The Ramsey spin-measurement SNR, the twist-untwist $\hat{J}_y$ SNR, the generator matrix element, and the QFI prefactors are analytical. Thus, the N^2 scaling in Eq. (31) follows analytically from the generator matrix element. Together, the universal factorization in Eq. (11), the analytical generator-dependent prefactors, and the numerical results in Fig. 2 provide a combined analytical and numerical validation of the asymptotic SNR expressions in Eqs. (30) and (31).

C. Effective information concentration: Optimal-information mode throws away most photons

We now discuss another remarkable feature of our optimized homodyne protocol: the optimized homodyne measurement involves a temporal mode whose average photon number scales *sublinearly* with the number of spins N. The implication is that for large N, even though we measure a tiny fraction of the emitted photons, we retrieve almost all of the information on φ in the initial state. An equivalent statement is that almost all of the output field can be discarded without degrading the precision of the estimation of φ.

TABLE I. Summary comparing the signal-to-noise ratio of ideal spin-ensemble measurements, which are experimentally challenging because of inefficient readout, with the SNR of the integrated homodyne current measured on the optimal temporal mode $w_{\mathrm{SNR}}(t)$ in Eq. (26). The table lists the large-N forms. These results, which hold asymptotically in N, are already approached for $N \sim \mathcal{O}(10^2)$.

Asymptotic SNR	$\hat{J}_\alpha$ meas.	Optimized homodyne
Standard Ramsey, Eq. (5)	N, Eq. (A4)	$\frac{N}{2}$, Eq. (30)
Twist-untwist, Eq. (6)	$\frac{N^2}{e}$, Eq. (A6)	$\frac{N^2}{2e}$, Eq. (31)

We can make the above statement more precise. Using Eq. (16), we compute the average photon number in the maximum-SNR temporal mode given in Eq. (26). We use this to define the *fractional occupation* of the maximum-SNR mode, $\bar{p}_{\mathrm{opt}}$, which varies from 0 to 1:

$$\bar{p}_{\mathrm{opt}} \equiv \frac{\bar{n}_{w_{\mathrm{SNR}}}}{N} = \frac{1}{N}\int_0^\infty \mathrm{d}t'\mathrm{d}t\, w_{\mathrm{SNR}}^{*}(t) g_1(t,t') w_{\mathrm{SNR}}(t'). \tag{32}$$

As shown in Fig. 4 (right panel), we find that the fractional occupation of the maximum-SNR mode decays as a power law with increasing N; numerical fits suggest a power law decay $\bar{p}_{\mathrm{opt}} \propto N^{-0.37}$, implying that the maximum SNR mode has an average photon number $\bar{n}_{\mathrm{opt}} \sim N^{0.63}$. We stress that this is also a "universal" result, as this scaling does not depend on the choice of the parameter generator $\hat{G}$.

We note that the small photon number (and hence power) associated with the optimal information mode could be advantageous in some experimental platforms, where one is perhaps worried about possible detector saturation effects associated with the large total photon number and power of the full superradiant burst. It is also worth stressing that there are many classical analogues of the behavior we find here, i.e., situations with structured Gaussian noise where the optimal matched filter yields a form that throws away most of the power in the detected field in order to exploit the presence of correlated noise. The difference in our setup is that this cancellation happens at the level of amplitudes and it stems from temporal correlations in the evolution of the system of spins, making this an effect of destructive quantum interference.

See Appendix I for more details about the interpretation of the optimal temporal mode of the radiation $w_{\mathrm{SNR}}(t)$.

D. Practical considerations

Here we briefly discuss the practical considerations relevant to potential experimental realizations of our general scheme. We first clarify what sets the phase reference for our optimal homodyne measurement. For

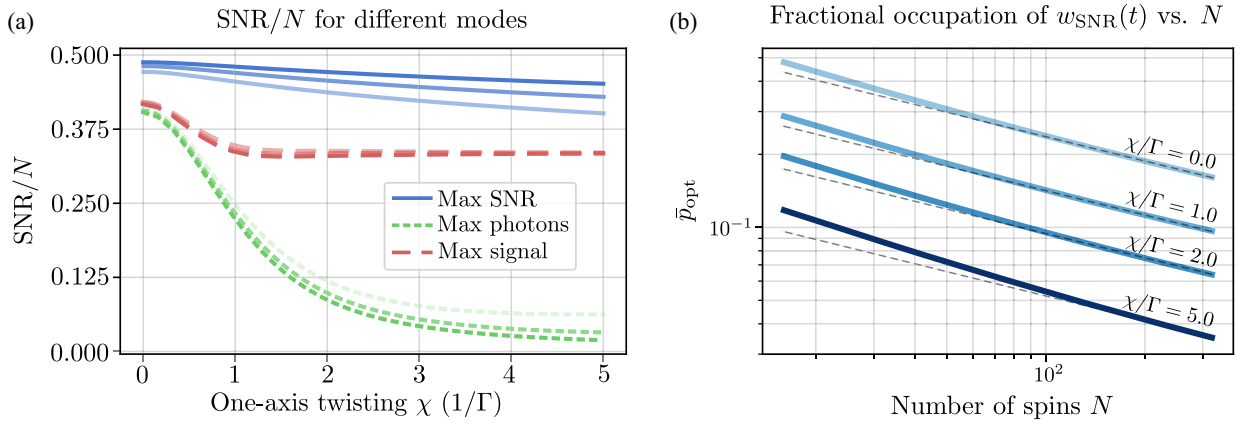


FIG. 4. (a) Homodyne SNR scaled by N for the three temporal modes $w_{\mathrm{SNR}}(t)$ (solid line), $w_{\mathrm{pop}}(t)$ (short dashed line), $w_{\mathrm{sig}}(t)$ (long dashed line) as a function of the spin-spin interaction χ produced by a detuned cavity; we consider the unentangled Ramsey-protocol initial state in Eq. (5). For large values of χ, there is a large difference between the SNR of the maximum-SNR mode and the naive maximum-photon mode. The opacity of the lines corresponds to different values of N ($N = 32, 64, 128$ for increasing opacity). Note that apart from an overall common scale factor, these curves are the same for any generator $\hat{G}$, and hence the figure also applies to the twist-untwist protocol which achieves Heisenberg scaling. (b) We plot the fractional occupation number in Eq. (32), for the maximum SNR mode in Eq. (26), for an ensemble of spins coupled to a detuned cavity. We fit the power law $r = aN^b$ to the results of the numerical computations, finding a consistent result for the exponent $b \simeq -0.37$ as the detuning is varied, and therefore the OAT term χ changes. The detuning through the OAT term has the effect of making the compression of the information in the few photons of the maximum-SNR mode even more evident.

standard homodyne protocols, one works with a coherently driven system, and hence there are natural amplitude and phase quadratures that are defined relative to the phase of the average input field amplitude $\langle \hat{b}_{\mathrm{in}} \rangle$. In such situations, the local oscillator reference is typically derived from the same laser (or source) used to generate the coherent drive $\hat{b}_{\mathrm{in}}$. In contrast, in our setup there is no coherent photonic driving, and hence no naturally defined amplitude and phase quadratures. Instead, the phase reference for the local oscillator will be determined by the same laser (or microwave source) used to encode information in the initial spin state. This encoding step is phase-sensitive, and the same drives that determine this encoding phase could be used to set the local-oscillator phase. Formally, the choice of the encoding phase is expressed in Eq. (11): the overall phase of the signal is determined by the phase of the matrix element $\langle m_0|\hat{G}|m_0 - 1\rangle$ of the generator $\hat{G}$. Note that, while photon counting has a vanishing linear sensitivity to a small rotation (since the mean photon number changes only quadratically with the rotation angle), it has the benefit that it does not require a shared phase reference.

Next, we would like to show that our scheme is robust against finite detection efficiency η. As is standard, we model a finite efficiency via an imbalanced beam-splitter, and the field entering homodyne detection by $\hat{b}_{\mathrm{det}} = \sqrt{\eta}\hat{b}_{\mathrm{out}} + \sqrt{1-\eta}\hat{b}_{\mathrm{vac}}$, with $\hat{b}_{\mathrm{vac}}$ the vacuum noise entering the second input port of the beam-splitter. Using this expression in the power SNR formula given in Eq. (22), we obtain

$$\mathrm{SNR}_{\eta}[u(t)] = \frac{\eta|\bar{S}_u|^2}{\eta \mathrm{Var}(\hat{M}_u) + (1-\eta)}. \tag{33}$$

In our case, the maximum SNR mode has an average photon number $\bar{n}_{\mathrm{opt}} \sim N^{\frac{2}{3}}$ and has no squeezing correlations. As such, the fluctuations of the max-SNR mode $\mathrm{Var}(\hat{M}_u)$ also scale as $\sim N^{\frac{2}{3}}$, and for $N \gg 1$ will completely dominate over the vacuum noise term in the denominator. This leads to $\mathrm{SNR}_{\eta} \approx \mathrm{SNR}_{\eta=1}$ if η is not too small.

Finally, we note that for large N, one does not need phase-sensitive detection schemes: a simple heterodyne scheme is also almost ideal (easily implemented in microwave systems using a standard IQ mixer). This would correspond to the above imperfect homodyne SNR expression with an efficiency $\eta = 0.5$. For large N, the same reasoning as above holds: the fluctuations of the max-SNR mode completely dominate the vacuum noise contribution associated with $\eta < 1$, and hence the heterodyne SNR is nearly the same as the homodyne SNR. A mismatch between the implemented temporal mode and the target filter reduces the SNR and changes the average photon number. In Appendix H, we show representative perturbation tests indicating that both the large SNR and the reduced photon number of the optimal mode are even more stable than expected against moderate timing offsets and errors in the assumed value of N. We have studied a representative metrological example for an $N = 128$ spin ensemble, and we have considered shifts in the applied mode of $\pm 10\%$ of the superradiant timescale, accompanied by perturbations $\Delta N \simeq \pm 30$ in the number of spins.

The simulations indicated reductions from the optimal SNR of only a few percent. The number of photons measured also remains well below that of the most populated mode.

V. INCLUDING COLLECTIVE SPIN-SPIN INTERACTIONS FROM CAVITY DETUNING

We now extend our analysis to cover collective dynamics that has the full form described by Eq. (2), i.e., both the collective superradiant decay dynamics and a cavity-mediated spin-spin interaction χ that has the form of a one-axis twisting Hamiltonian. This detuned regime is not just a theoretical curiosity: in many systems with large N, the resonant case would produce a collective decay rate Γ that is too fast to be experimentally accessed. In such cases, a small detuning Δ could be used to slow down the superradiant decay to be more compatible with accessible timescales. While a detuning will reduce the value of Γ, it also modifies the dynamics as there is now a Hamiltonian spin-spin interaction. We study here whether this modification degrades our basic homodyne measurement strategy. As we show, the answer is no: an optimized homodyne measurement (using a simple linear estimator) still achieves excellent performance. The OAT interaction does not modify the characteristic timescale of the burst, defined by the rapid inversion of $\langle \hat{J}_z \rangle$. Because of the weak $U(1)$ symmetry under rotations about $\hat{J}_z$, the Dicke-state populations obey a set of differential equations that is decoupled from the coherences. The interaction proportional to χ affects only the coherences and therefore does not modify the population dynamics or the timing of the burst. We have verified this independence from χ numerically.

We repeat the generic mode analysis of the previous sections for dynamics that includes a non-zero interaction χ. One finds changes already at the level of how photons are distributed in the output field. As χ/Γ becomes appreciable, the photon population becomes less concentrated on just a single mode. We can again use Eqs. (17), (21), and (26) to compute the modes that optimize the average photon number, the net integrated signal, and, most interestingly, the homodyne SNR. The results for how the SNRs of these modes behave are shown in Fig. 4, for an initial unentangled spin state corresponding to a Ramsey protocol [cf. Eq. (5)]. While the SNRs of the maximum-signal and maximum-SNR modes are comparable, the SNR of the most populated mode rapidly drops when the detuning is increased. Because of the factorization in Eq. (28), the same functional dependence of the SNR on χ reported in Fig. 4 would be valid for every generator $\hat{G}$, when appropriately rescaled by $|\langle m_0|\hat{G}|m_0-1\rangle|^2$.

We can also study the "concentration" effect we found for the resonant-cavity case, where the maximum-SNR mode contains a vanishing fraction of the total emitted photons. We compute numerically the ratio in Eq. (32) for multiple values of the OAT interaction strength χ, each time fitting the decay of the fractional occupation $\bar{p}_{\mathrm{opt}}$ with N to a power law. We observe that the decay exponent varies weakly with the value of χ, with a steeper decay with increasing χ. This implies that the "concentration" effect is even more pronounced in the case where there are non-zero spin-spin interactions.

While the optimized modes $w_{\mathrm{pop}}(t)$, $w_{\mathrm{sig}}(t)$, and $w_{\mathrm{SNR}}(t)$ are all real for $\chi = 0$, they become complex functions when the detuning is increased, i.e., $\chi \neq 0$. This implies that the quadrature to measure in the optimal homodyne detection changes non-trivially with time, on the timescale of the (slowed) superradiant emission, making the experimental realization more challenging.

VI. BEYOND LINEAR ESTIMATION: RECOVERING THE FULL QUANTUM FISHER INFORMATION USING HOMODYNE MEASUREMENT

Our analysis of homodyne measurement has focused so far exclusively on the simplest experimental protocol, where the estimate of the parameter φ is proportional to the measured, filtered homodyne current associated with a given temporal mode. As discussed, the shape of the maximum-SNR mode we found in Eq. (26) and the corresponding maximum value of the SNR are given by expressions that match the theory of classical generalized matched filters. One can easily show that *if* the homodyne current could be accurately modeled as a Gaussian stochastic process (i.e., its fluctuations involve no higher-order cumulants), then the linear estimator we use would be optimal, and the SNR we calculate would be the full Fisher information associated with the homodyne current $I(t)$. This then raises an interesting question: is there an appreciable non-Gaussian character to the fluctuations of the homodyne current? If there are higher cumulants, can these be used to improve the parameter estimation beyond what is possible with a simple linear estimator? We show that, surprisingly, the answer to both these questions is positive.

In particular, for the resonant-cavity setup ($\chi = 0$), the classical Fisher information of the homodyne current saturates the QFI of the initial spin-ensemble state. This can only happen if the current has appreciable non-Gaussianity; otherwise, it would be limited to half of the QFI. We show this result by introducing a novel equivalence between the light emitted by the ensemble in our setup (where the parameter is encoded in the initial state of the spins) and a continuous-metrology protocol [61], where the parameter φ controls the form of the Lindbladian that governs dynamics. This rigorous equivalence allows us to employ a modified version of the conditions recently formulated in Ref. [34] to show that the full information content of a homodyne measurement

(its CFI) saturates the bound set by the QFI of the output field. While in Ref. [34] the saturation of the QFI for a Hamiltonian encoding is studied, we deal with the case of a parameter encoded by the dissipative part of the spin evolution.

Comparing this result with our results for the SNR, we conclude that non-Gaussian correlations in the homodyne current remain metrologically relevant as $N \to \infty$. In fact, we can define a Gaussian stochastic process with average $\mu_\varphi(t) \equiv \langle \hat{I}(t) \rangle_\varphi$, having covariance matrix given by Eq. (13). We restrict to the resonant scenario, so that both the signal $\alpha_I(t)$ and the fluctuation matrix are real. To define the Gaussian process, we fix a time-independent quadrature for the homodyne detection, i.e., $\theta = \text{const}$ in Eq. (12). In this scenario the CFI of the Gaussian process is exactly the SNR of the linear measurement reported in Eq. (27). In summary, the optimal estimator that considers the fluctuations of the current as Gaussian achieves half of the QFI, but we know that considering the full set of correlations in the trajectories would give the full QFI. This means that there are non-Gaussian correlations in the current.

While this result on the full CFI of the homodyne current is both interesting and surprising, making use of it experimentally would require potentially complex processing of the full time-dependent homodyne current. We stress that the much simpler protocol studied in the main text (based on a simple linear estimator) already comes within a factor of two of the full output-field QFI.

VII. CONCLUSIONS

We can summarize the results of our work with two key take-home points:

(1) Filtered homodyne detection with a simple linear estimator is almost optimal for extracting information from a superradiant burst generated by a spin ensemble whose initial state encodes a parameter of interest. The signal-to-noise ratio of such an estimator is only a factor $\simeq 2$ away from the fundamental bound set by the quantum Fisher information. This result holds for a surprisingly broad class of parameter generators; in particular, it holds for cases where there is Heisenberg scaling in the number of spins N.

(2) A vanishingly small fraction of all the photons in the photonic output field generated by superradiance carries almost all the information encoded in the initial spin state (implying an effective kind of compression of information).

While our work emphasizes the fundamental aspects of our general setup, we stress that our results could enable a new method for using cavities to read out information stored in a spin ensemble. Compared to a conventional dispersive readout, the superradiant readout we describe does not require any detuning and hence makes use of the full spin-photon coupling. This could be advantageous in sensing platforms where solid-state spin ensembles couple to microwave cavities. Because coupling strengths are weak in these systems, a resonant approach could be highly beneficial.

Our work also suggests many additional intriguing theory investigations. For example, could control operations be applied to the spins to influence and perhaps enhance the information of the output state? Could similar ideas to what we describe be employed in superradiant decay phenomena involving ordered arrays of emitter spins, in the absence of a cavity? It would also be interesting to develop a more complete understanding of our surprising finding that the maximum SNR mode contains a vanishing fraction of the emitted photons. Can one identify an underlying mechanism and perhaps generalize it to a broader class of systems where this effective compression might be useful?

VIII. CODE AVAILABILITY

All the code used to perform the simulations will be made available in a repository upon publication of the manuscript.

ACKNOWLEDGMENTS

This material is based upon work supported by the U.S. Department of Energy Office of Science National Quantum Information Science Research Centers as part of the Q-NEXT center. Q-NEXT provided primary funding support for F. B. during the completion of this research. A. C. acknowledges support from the Simons Foundation through a Simons Investigator Award (Grant No. 669487).

DATA AVAILABILITY

There are no publicly available research data or software supporting this manuscript. Requests for further information or data should be sent to the authors.

APPENDIX A: ANALYTICAL SPIN-MEASUREMENT BENCHMARKS AND GENERATOR PREFACTORS

In this appendix, we collect the quantum Fisher information for the Ramsey and twist-untwist protocols, together with the generator matrix elements entering the factorized homodyne SNR in Eq. (28).

For Ramsey encoding, $\hat{G}_S = \hat{J}_y$, and the pure-state QFI is

$$\begin{aligned} \mathcal{F}_\varphi(|\psi_\varphi^S\rangle) &= 4\left[\langle m_0|\hat{J}_y^2|m_0\rangle - \langle m_0|\hat{J}_y|m_0\rangle^2\right] \\ &= N. \end{aligned} \tag{A1}$$

For the twist-untwist state, let $\mu \equiv Q/N$ and $\hat{G}_E \equiv \hat{U}_s^\dagger \hat{J}_y \hat{U}_s$. The QFI can be evaluated exactly for arbitrary Q:

$$\mathcal{F}_\varphi(|\psi_\varphi^E\rangle) = N + \frac{N(N-1)}{2}[1-\cos^{N-2}(2\mu)]. \quad \text{(A2)}$$

For the value Q_{opt} used in the main text, this becomes

$$\mathcal{F}_\varphi(|\psi_\varphi^E\rangle) = N + \frac{N(N-1)}{2}\left[1-\left(\frac{N-3}{N-1}\right)^{N-2}\right] \sim \frac{1-\mathrm{e}^{-2}}{2}N^2, \quad \text{(A3)}$$

for large N. For the unentangled state $|\psi_\varphi^S\rangle$, a simple projective measurement and linear estimator are optimal. This can be seen explicitly by computing the signal-to-noise ratio associated with a projective $\hat{J}_x$ measurement:

$$\mathrm{SNR}(|\psi_\varphi^S\rangle;\hat{J}_x) = \frac{|\langle m_0|[\hat{J}_y,\hat{J}_x]|m_0\rangle|^2}{\langle m_0|\hat{J}_x^2|m_0\rangle} = N. \quad \text{(A4)}$$

The SNR coincides with the full QFI of the state, indicating that projective measurements with a linear estimator are ideal.

We contrast this result with the case of the twist-untwist state $|\psi_\varphi^E\rangle$. In this case, the optimal spin component to measure is $\hat{J}_y$, and we find that the SNR for a projective measurement is

$$\mathrm{SNR}(|\psi_\varphi^E\rangle;\hat{J}_y) = N(N-1)^2\sin^2\mu\,\cos^{2N-4}\mu. \quad \text{(A5)}$$

Maximizing Eq. (A5) gives $\tan^2\mu_{\text{opt}} = 1/(N-2)$, i.e., $Q_{\text{opt}} = N\arctan[1/\sqrt{N-2}]$. For $Q = Q_{\text{opt}}$, this gives the exact finite-N result

$$\mathrm{SNR}(|\psi_\varphi^E\rangle;\hat{J}_y) = N(N-1)\left(\frac{N-2}{N-1}\right)^{N-2} \sim \frac{N^2}{e} \simeq 0.85\ \mathcal{F}_\varphi(|\psi_\varphi^E\rangle) \quad \text{as } N\to\infty. \quad \text{(A6)}$$

The asymptotic regime is achieved already for $N \sim \mathcal{O}(10^2)$. In Ref. [31], it has been proven that this is indeed the maximum SNR for the twist-untwist strategy with a linear estimator. Hence, we see that, in this case, a simple projective measurement (and a linear estimator) allows one to achieve Heisenberg scaling, but it does not saturate the QFI. If we were to consider the full statistics of the outcomes of the measurement on $\hat{J}_y$, then we could saturate the QFI asymptotically in the number of spins. The optimal measurement can be computed from the theory of quantum metrology as the projector onto the eigenvectors of the symmetric logarithmic derivative; see Ref. [62].

Finally, we give the generator prefactors that multiply the universal fluctuation integral in Eq. (28). For Ramsey encoding,

$$\langle m_0|\hat{G}_S|m_0-1\rangle = -\frac{i\sqrt{N}}{2}, \qquad |\langle m_0|\hat{G}_S|m_0-1\rangle|^2 = \frac{N}{4}. \quad \text{(A7)}$$

For twist-untwist encoding at $Q = Q_{\text{opt}}$, the corresponding squared matrix element is

$$|\langle m_0|\hat{G}_E|m_0-1\rangle|^2 = \frac{N}{4}\frac{N^2-N-1}{N-1}\left(\frac{N-2}{N-1}\right)^{N-2} \sim \frac{N^2}{4e}. \quad \text{(A8)}$$

Combining these analytical prefactors with the universal fluctuation-dependent integral in Eq. (28) gives the homodyne results quoted in Eqs. (30) and (31).

APPENDIX B: COMPUTATION OF THE HOMODYNE SIGNAL FOR THE SPIN ENSEMBLE

Throughout this appendix, we restrict the explicit signal evolution to the resonant case $\chi = 0$. Let us start with the definition of $\alpha_I(t)$ in Eq. (9),

$$\alpha_I(t) = -\sqrt{\Gamma}\langle m_0|[\hat{G},\hat{J}_-(t)]|m_0\rangle. \quad \text{(B1)}$$

We reformulate the expectation value of the commutator:

$$\langle[\hat{G},\hat{J}_-(t)]\rangle = \mathrm{Tr}\Big(\hat{\rho}[\hat{G},\hat{J}_-(t)]\Big) \quad \text{(B2)}$$

$$= \mathrm{Tr}\Big(\hat{\rho}\hat{G}\hat{J}_-(t) - \hat{G}\hat{\rho}\hat{J}_-(t)\Big) \quad \text{(B3)}$$

$$= \mathrm{Tr}\Big([\hat{\rho},\hat{G}]\hat{J}_-(t)\Big) \quad \text{(B4)}$$

$$= \mathrm{Tr}\Big(\mathrm{e}^{\mathcal{D}[\sqrt{\Gamma}\hat{J}_-]t}\Big([\hat{\rho},\hat{G}]\Big)\hat{J}_-\Big). \quad \text{(B5)}$$

We assume that the generator $\hat{G}$ of the signal is collective, i.e., it is entirely defined as an operator by its matrix elements in the symmetric subspace:

$$\hat{G} = \sum_{m',m=-m_0}^{m_0}\langle m'|\hat{G}|m\rangle|m'\rangle\langle m| \equiv \sum_{m',m}G_{m',m}|m'\rangle\langle m|, \quad \text{(B6)}$$

with $m_0 = \frac{N}{2}$. The commutator $[\hat{\rho},\hat{G}]$ can therefore be expressed as

$$[\hat{\rho},\hat{G}] = |m_0\rangle\langle m_0|\left(\sum_{m',m=-m_0}^{m_0} G_{m',m}|m'\rangle\langle m|\right) - \left(\sum_{m',m=-m_0}^{m_0} G_{m',m}|m'\rangle\langle m|\right)|m_0\rangle\langle m_0|, \tag{B7}$$

which yields

$$\hat{X}(t=0) \equiv [\hat{\rho},\hat{G}] = \sum_{m=-m_0}^{m_0} G_{m_0,m}|m_0\rangle\langle m| - \sum_{m=-m_0}^{m_0} G_{m,m_0}|m\rangle\langle m_0|. \tag{B8}$$

This operator admits the matrix representation

$$\hat{X}(t=0) \equiv \begin{bmatrix} 0 & 0 & 0 & \cdots & -G_{-m_0,m_0} \\ 0 & 0 & 0 & \ddots & \vdots \\ 0 & 0 & 0 & \ddots & -G_{m_0-2,m_0} \\ \vdots & \ddots & \ddots & \ddots & -G_{m_0-1,m_0} \\ G_{m_0,-m_0} & \cdots & G_{m_0,m_0-2} & G_{m_0,m_0-1} & 0 \end{bmatrix}. \tag{B9}$$

We define the time-evolved commutator

$$\hat{X}(t) = e^{\mathcal{D}[\sqrt{\Gamma}\hat{J}_-]t}([\hat{\rho},\hat{G}]) = \begin{bmatrix} 0 & \square & \square & \cdots & \square \\ \blacksquare & 0 & \square & \ddots & \vdots \\ \square & \blacksquare & 0 & \ddots & \square \\ \vdots & \ddots & \ddots & \ddots & \square \\ \square & \cdots & \square & \blacksquare & 0 \end{bmatrix}. \tag{B10}$$

This evolution does not introduce any extra coherence in the system, which also implies that the operator $\hat{X}(t)$ has zeros on the diagonal. Note that the presence of a Hamiltonian term $\hat{H} = \chi\hat{J}_z^2$, which may originate from detuning the spins from the cavity, has the effect of adding a time-dependent phase to all off-diagonal matrix elements. However, this does not change the structure of Eq. (B10) and it will not change our conclusions in this section. The explicit evolution in Eq. (B12) below is nevertheless restricted to the resonant case $\chi = 0$. The multiplication by

$$\hat{J}_- = \sum_{m=-m_0}^{m_0} \sqrt{m_0(m_0+1) - m(m-1)}\,|m-1\rangle\langle m| \tag{B11}$$

selects only the subdiagonal elements of the time-evolved commutator as the terms that contribute to the homodyne signal $\alpha_I(t)$; these terms have been indicated by the black boxes in Eq. (B10). Therefore, we only need to track the evolution of the N elements of the subdiagonal of the commutator, which we denote by $X_m(t)$ for $m = -m_0, -m_0+1, \cdots, m_0-1$. These elements satisfy the differential equation

$$\frac{dX_m(t)}{dt} = -\frac{1}{2}(\Gamma_m + \Gamma_{m+1})X_m(t) + \sqrt{\Gamma_{m+2}\Gamma_{m+1}}X_{m+1}(t), \tag{B12}$$

with $\Gamma_m \equiv \Gamma(m+m_0)(m_0-m+1)$, and $X_{m_0}(t) \equiv 0,\ \forall\ t$ by definition. The initial condition is

$$X_m(t=0) = \delta_{m,m_0-1}G_{m_0,m_0-1}. \tag{B13}$$

The final expression for the homodyne signal is

$$\alpha_I(t) = -\sqrt{\Gamma}\sum_{m=-m_0}^{m_0-1} X_m(t)\sqrt{(m+m_0+1)(m_0-m)}. \tag{B14}$$

APPENDIX C: PROOF OF THE SEPARATION THEOREM

1. Separation theorem without cavity

We will now prove that the homodyne signal for an ensemble of spins starting in the fully excited state is factorized, as written in Eq. (11). This statement follows from Eq. (B14) in Appendix B: The expression for the signal involves $X_m(t)$, which evolves linearly in time from an initial condition proportional to a single entry of the signal generator G, see Eqs. (B13) and (B12); we can indeed write

$$X_m(t=0) = G_{m_0,m_0-1}\tilde{X}_m(t=0), \tag{C1}$$

with $\tilde{X}_m(t=0) = \delta_{m,m_0-1}$ and $G_{m_0,m_0-1} \equiv \langle m_0|\hat{G}|m_0-1\rangle$. The renormalized vector $\tilde{X}(t)$ evolves according to the same equation of motion reported in Eq. (B12) for $X(t)$. By linearity we can write the expression for the homodyne signal as a function of $\tilde{X}_m(t)$:

$$\alpha_I(t) = -\sqrt{\Gamma}G_{m_0,m_0-1} \times \sum_{m=-m_0}^{m_0-1} \tilde{X}_m(t)\sqrt{(m+m_0+1)(m_0-m)}, \tag{C2}$$

which proves the theorem with

$$\tilde{\alpha}_I(t) \equiv -\sqrt{\Gamma}\sum_{m=-m_0}^{m_0-1} \tilde{X}_m(t)\sqrt{(m+m_0+1)(m_0-m)}. \tag{C3}$$

2. Separation theorem with cavity

In this subsection, we prove the same separation statement on $\alpha_I(t)$ for a system with a cavity that has not been adiabatically eliminated. We are able to prove the separation theorem for any collective spin Hamiltonian $\hat{H}_s$ satisfying $[\hat{H}_s, \hat{J}_z] = 0$. We assume the interaction term between the cavity and the spins to be that of the Tavis-Cummings model in Eq. (1), while the cavity loss is described by the superoperator

$$\mathcal{D}[\sqrt{\kappa}\hat{a}](\hat{X}) \equiv \kappa\left(\hat{a}\hat{X}\hat{a}^\dagger - \frac{1}{2}\{\hat{a}^\dagger\hat{a}, \hat{X}\}\right). \tag{C4}$$

We will use the shortened notation $|m\rangle \equiv |j = N/2, m\rangle$, because the spin ensemble remains in the symmetric subspace during the evolution, since the interaction with the cavity is collective and we assume a collective Hamiltonian. We denote by $|n\rangle$ the Fock state of the cavity, and by $|m, n\rangle$ the joint state of the spins and the cavity containing n photons. We start by analyzing the evolution of an operator $\hat{X}(t = 0) \equiv |M, N\rangle\langle M', N'|$, under the Tavis-Cummings model. If the total energy of the spins and the cavity is conserved, in the evolved operator $\hat{X}(t)$, which we write as

$$\hat{X}(t) = \sum_{\substack{n,m \\ n',m'}} X_{n'm',nm}(t)|m, n\rangle\langle m', n'|, \tag{C5}$$

only those terms satisfying

$$m + n = M + N, \qquad m' + n' = M' + N', \tag{C6}$$

can have a non-zero coefficient. We now consider also the loss term and we evolve $\hat{X}(t)$ under the master equation for the decaying ensemble of spins. The anticommutator with the photon number in Eq. (C4) acts on each operator $|m, n\rangle\langle m', n'|$ by sending it to $(n + n')|m, n\rangle\langle m', n'|$ and therefore does not create new non-zero terms in the evolution of $\hat{X}(t)$, and in particular it is energy preserving. On the other hand, $\hat{a}\hat{X}\hat{a}^\dagger$ is not energy preserving and it destroys quanta of energy on both the kets and bras of $|m, n\rangle\langle m', n'|$. The application of the Hamiltonian term again exchanges energy between the cavity and the spins, so that as a whole the energy of the system (ensemble and cavity) can only decrease, but separately for the kets and the bras of the generic operator $\hat{X}(t)$. We conclude that in evolving $\hat{X}(t)$ we can have only non-zero coefficients $X_{n'm',nm} \neq 0$ if the indices satisfy

$$m + n \leq M + N, \qquad m' + n' \leq M' + N'. \tag{C7}$$

The final key observation is that in the photon loss process described by Eq. (C4), two quanta of energy are annihilated at the same time on the left and on the right of $|m, n\rangle\langle m', n'|$, which implies that the difference in the number of excitations (between cavity and spins) on the bras and the kets must remain constant. We have therefore the additional constraint

$$m + n - (n' + m') = M + N - (N' + M'). \tag{C8}$$

We now introduce an expression for the homodyne signal $\alpha_I(t)$, analogous to Eq. (9), but without the adiabatic elimination of the cavity. Starting from the input-output relation

$$\hat{b}_{\text{out}}(t) = \sqrt{\kappa}\hat{a}(t) + \hat{b}_{\text{in}}(t), \tag{C9}$$

we can write

$$\alpha_I(t) = -i\sqrt{\kappa}\langle[\hat{G} \otimes \mathbb{I}, \hat{a}(t)]\rangle. \tag{C10}$$

The generator of the encoding $\hat{G}$ acts only on the spins, while $\hat{a}(t)$ is the evolved decay operator acting both on the spins and the cavity mode. We focus on the computation of $\langle[\hat{G} \otimes \mathbb{I}, \hat{a}(t)]\rangle$, from which the full homodyne signal $\alpha_I(t)$ can be obtained. This term can be rewritten as

$$\langle[\hat{G} \otimes \mathbb{I}, \hat{a}(t)]\rangle = \text{Tr}\left(\hat{X}(t)\hat{a}\right), \tag{C11}$$

where the operator $\hat{X}(t)$ is the evolution of the commutator $[\hat{\rho} \otimes |0\rangle\langle 0|, \hat{G} \otimes \mathbb{I}]$, with the Lindbladian evolution $e^{\mathcal{L}t}$ for the dissipative Tavis-Cummings model, constructed with the Hamiltonian in Eq. (1) together with $\hat{H}_s$ satisfying $[\hat{H}_s, \hat{J}_z] = 0$, and the dissipator in Eq. (C4), i.e.,

$$\hat{X}(t) = \text{e}^{\mathcal{L}t}\left([\hat{\rho} \otimes |0\rangle\langle 0|, \hat{G} \otimes \mathbb{I}]\right). \tag{C12}$$

We work under the assumption that the initial state of the spins is $\hat{\rho} \equiv |m_0\rangle\langle m_0|$, and that the cavity is initially in the vacuum state, so that we can specify the commutator:

$$[\hat{\rho} \otimes |0\rangle\langle 0|, \hat{G} \otimes \mathbb{I}] = \underbrace{\sum_{M'=-m_0}^{m_0} |m_0, 0\rangle\langle M', 0|G_{m_0,M'}}_{\text{I}} - \underbrace{\sum_{M=-m_0}^{m_0} G_{M,m_0}|M, 0\rangle\langle m_0, 0|}_{\text{II}}. \tag{C13}$$

We also write the lowering operator of the cavity in the Fock basis, while adding explicitly the identity on the spins:

$$\mathbb{I}\otimes\hat{a}=\left(\sum_{m=-m_0}^{m_0}|m\rangle\langle m|\right)\otimes\left(\sum_{n=0}^{\infty}\sqrt{n}\,|n-1\rangle\langle n|\right). \tag{C14}$$

Let us consider the evolved version of the operator in Eq. (C13). We will focus only on those matrix elements that produce a non-zero value when contracted with $\mathbb{I}\otimes\hat{a}$. We divide this analysis into the elements of summands I and II in Eq. (C13).

(i) $m+n-m'-n'=j-M'$. In order for $|m,n\rangle\langle m',n'|$ to give a non-zero signal in $\mathrm{Tr}(|m,n\rangle\langle m',n'|\,\hat{a})$, we need $n-n'=1$ and $m=m'$, which fixes $M'=j-1$, i.e., only a single operator in the first summation is non-zero.

(ii) $m+n-m'-n'=M-j$. The same analysis gives $M=j+1$, which is out of the range of the summation, and it means that the contribution of II to the homodyne signal is zero.

We conclude that the homodyne signal is

$$\alpha_I(t)=-i\sqrt{\kappa}G_{m_0,m_0-1}\mathrm{Tr}[e^{\mathcal{L}t}(|m_0,0\rangle\langle m_0-1,0|)\cdot\hat{a}],$$

which proves the separation theorem.

APPENDIX D: DEFINITIONS OF THE ESTIMATOR AND ITS PERFORMANCE

In this appendix, we define the relevant local information quantities we use to establish the metrological performance of our homodyne detection protocol. We consider measuring a Hermitian observable $\hat{M}\equiv\int_{\mu\in\mathcal{M}}\mathrm{d}\mu\,\mu|\mu\rangle\langle\mu|$ on the state $\hat{\rho}_R^{\varphi}(t)$ of the output field at time t, which carries a dependence on φ. We denote by $\mu\in\mathcal{M}$ the different possible measurement outcomes, which are observed with probability

$$p(\mu|\varphi)\equiv\mathrm{Tr}(\hat{\rho}_R^{\varphi}(t)|\mu\rangle\langle\mu|). \tag{D1}$$

We omit the time dependence in the probability distribution $p(\mu|\varphi)$ to make the notation easier. The value of the parameter φ that is encoded in the state of the spins by the unitaries in Eqs. (5) and (6) is $\varphi=\varphi_0$. Since we work in the regime of local estimation, we will study the estimation of small deviations of the parameter φ from the reference value φ_0. For clarity, we distinguish between the encoded parameter φ and its value φ_0 in this section. In the rest of the manuscript, however, we drop the subscript in φ_0 and use the symbol φ also for the actual value encoded in the spin ensemble. While in this section we consider observables measured on the state of the radiation field, it is always possible to reexpress them as expectation values measured on the state of the spins by means of the input-output theory, as we do throughout the manuscript and in the appendix (see also [59]). The expectation value of an arbitrary Hermitian observable $\hat{A}$ with respect to $\hat{\rho}_R^{\varphi}(t)$ is $\langle\hat{A}\rangle_{\varphi}\equiv\mathrm{Tr}(\hat{A}\hat{\rho}_R^{\varphi}(t))$ (where, again, we omit the time dependence for the sake of clarity). The average of the observable $\hat{M}$ and its square $\hat{M}^2$ can then be expressed as

$$\langle\hat{M}\rangle_{\varphi}=\int_{\mu\in\mathcal{M}}\mathrm{d}\mu\,\mu\,p(\mu|\varphi), \tag{D2}$$

$$\langle\hat{M}^2\rangle_{\varphi}=\int_{\mu\in\mathcal{M}}\mathrm{d}\mu\,\mu^2\,p(\mu|\varphi). \tag{D3}$$

The variance of the observable is defined as

$$\mathrm{Var}(\hat{M})_{\varphi}\equiv\langle\hat{M}^2\rangle_{\varphi}-\langle\hat{M}\rangle_{\varphi}^2 \tag{D4}$$

$$=\mathbb{E}_{\varphi}[\mu^2]-(\mathbb{E}_{\varphi}[\mu])^2, \tag{D5}$$

where the expectation value over $p(\mu|\varphi)$ is

$$\mathbb{E}_{\varphi}[\cdot]\equiv\int_{\mu\in\mathcal{M}}\mathrm{d}\mu\cdot p(\mu|\varphi). \tag{D6}$$

In the following, we explicitly restrict to a single measurement of $\hat{M}$ and denote the corresponding random outcome by μ. A locally unbiased estimator [63] for the parameter of interest at the position φ_0 can then be constructed directly from μ, i.e.,

$$\breve{\varphi}\equiv\left(\frac{\partial\langle\hat{M}\rangle_{\varphi}}{\partial\varphi}\bigg|_{\varphi=\varphi_0}\right)^{-1}(\mu-\langle\hat{M}\rangle_{\varphi_0})+\varphi_0, \tag{D7}$$

which is sensitive to deviations from the reference value φ_0. It is easy to verify

$$\mathbb{E}_{\varphi_0}[\breve{\varphi}]=\varphi_0\quad\text{and}\quad\frac{\partial\mathbb{E}_{\varphi}[\breve{\varphi}]}{\partial\varphi}\bigg|_{\varphi=\varphi_0}=1,$$

which are the conditions for local unbiasedness. For the single-shot estimator considered here, the variance at φ_0 is the inverse of the signal-to-noise ratio:

$$\mathrm{Var}(\breve{\varphi})_{\varphi_0}=\frac{1}{\mathrm{SNR}},\qquad\mathrm{SNR}\equiv\frac{\left|\frac{\partial\langle\hat{M}\rangle_{\varphi}}{\partial\varphi}\right|^2_{\varphi=\varphi_0}}{\mathrm{Var}(\hat{M})_{\varphi_0}}. \tag{D8}$$

Upper bounds on the SNR are the classical Fisher information (CFI, computed from the classical probability distribution $p(\mu|\varphi)$) and the quantum Fisher information (QFI) of $\hat{\rho}_R^{\varphi}(t)$ (obtained by maximizing the CFI over all possible measurements), both evaluated at φ_0 [51]. The QFI will be our reference value for the maximum amount of information that can be extracted from the radiation. Note that the joint evolution of the spins, the cavity, and the radiation field is unitary and the encoding happens entirely before the decay. Therefore, in the absence of unobserved

decay channels, the QFI of the state of the radiation field long after the decay has ended must be equal to the QFI of the spin ensemble right after the encoding, i.e., the QFI of the state given in Eq. (3). The corresponding Cramér-Rao bound is therefore the same whether it is expressed for measurements on the initially encoded spin state or for measurements on the full emitted field.

For a homodyne detection measurement, we have $\hat{M} = \hat{M}_u$ as defined in Eq. (19).

APPENDIX E: DERIVATION OF THE PHOTON NUMBER SENSITIVITY

In this appendix we calculate the sensitivity of a photon counting measurement applied to a single mode of the radiation emitted by the spin ensemble. The expressions derived in this section are applicable to every generator $\hat{G}$ of the parameter φ. The temporal-mode formalism allows us to classify the temporal modes of the radiation field according to their sensitivity under a photon-counting measurement. We show that for a superradiant ensemble of spins initialized in the fully excited state, the sensitivity of the photon number is always zero for any metrological generator $\hat{G}$. Our analysis mirrors the derivation in Ref. [59].

Parametric derivative of the correlation function. We compute the sensitivity of the photon number in a generic mode. We introduce explicitly the dependence of the photon number on φ, and we write the average number of photons in a temporal mode of the output field:

$$\bar{n}_u(\varphi) \equiv \langle \hat{b}_u^\dagger \hat{b}_u \rangle_\varphi = \int_0^\infty \mathrm{d}t' \mathrm{d}t\, u^*(t') g_1(t', t; \varphi) u(t). \quad \text{(E1)}$$

Here, $g_1(t', t; \varphi) \equiv \Gamma \langle \hat{J}_+(t') \hat{J}_-(t) \rangle_\varphi$. The expectation value is $\langle \cdot \rangle_\varphi \equiv \langle \Psi_\varphi | \cdot | \Psi_\varphi \rangle$, or equivalently $\langle m_0 | \hat{U}_\varphi^\dagger \cdot \hat{U}_\varphi | m_0 \rangle$ after suppressing the vacuum input field. The sensitivity of the photon number to variations of φ is gauged by the derivative

$$\left.\frac{\partial \bar{n}_u(\varphi)}{\partial \varphi}\right|_{\varphi=0} = \int_0^\infty \mathrm{d}t' \mathrm{d}t\, u^*(t') \left.\frac{\partial g_1(t', t; \varphi)}{\partial \varphi}\right|_{\varphi=0} u(t). \quad \text{(E2)}$$

It contains the parametric derivative of the correlation function with respect to φ,

$$\left.\frac{\partial g_1(t', t; \varphi)}{\partial \varphi}\right|_{\varphi=0} = -i\Gamma \langle [\hat{G}, \hat{J}_+(t') \hat{J}_-(t)] \rangle, \quad \text{(E3)}$$

with the expectation value taken in the unencoded initial state $|\Psi_0\rangle$. This expression has the form of a linear-response function for the operator $\hat{J}_+(t')\hat{J}_-(t)$ under a small perturbation generated by $\hat{G}$. Let us denote by $\hat{\rho} = |m_0\rangle\langle m_0|$ the initial, unencoded state of the spins. Then we can rewrite the derivative as follows.

$$\left.\frac{\partial g_1(t', t; \varphi)}{\partial \varphi}\right|_{\varphi=0} = -i\Gamma \,\mathrm{Tr}\Big(\hat{\rho}[\hat{G}, \hat{J}_+(t') \hat{J}_-(t)]\Big) \quad \text{(E4)}$$

$$= -i\Gamma \,\mathrm{Tr}\Big([\hat{\rho}, \hat{G}] \hat{J}_+(t') \hat{J}_-(t)\Big). \quad \text{(E5)}$$

We will use this expression in the following paragraph to prove that the sensitivity of the mode photon-number measurement with linear estimators is always zero. This result tells us that, with the exception of pathological cases where both the signal and the noise tend to zero at the same rate (which are not practical from an experimental point of view), the photon counting measurement with a linear estimator is never useful in superradiant metrology.

Sensitivity of the photon counting measurement. We can compute the expression in Eq. (B10) by evaluating the evolution of the commutator $[\hat{\rho}, \hat{G}]$, which is given by the expression in Eq. (B8). Given the time-evolved operator $\hat{X}(t')$ and $\hat{J}_-$,

$$\hat{X}(t') = \sum_{m', m=-m_0}^{m_0} X_{m'm}(t') |m'\rangle\langle m| \quad \text{(E6)}$$

$$\hat{J}_- = \sum_{m=-m_0}^{m_0} \sqrt{m_0(m_0+1) - m(m-1)}\, |m-1\rangle\langle m|, \quad \text{(E7)}$$

we evaluate $\hat{J}_- X(t')$,

$$\hat{J}_- \hat{X}(t') = \left(\sum_{m''=-m_0}^{m_0} \sqrt{m_0(m_0+1) - m''(m''-1)}\, |m''-1\rangle\langle m''| \right) \cdot \left(\sum_{m', m=-m_0}^{m_0} X_{m'm}(t') |m'\rangle\langle m| \right), \quad \text{(E8)}$$

which, simplified, leaves us with

$$\hat{J}_- \hat{X}(t') = \sum_{m, m'=-m_0}^{m_0} \sqrt{m_0(m_0+1) - m'(m'-1)} \cdot X_{m'm}(t') |m'-1\rangle\langle m|. \quad \text{(E9)}$$

This operator then must be evolved until time t. Because $X_{mm}(t) = 0$, the sub-diagonal with $m' = m$ of $\hat{J}_-\hat{X}(t')$ remains zero. We can therefore write the evolved state as

$$\hat{Y} = \mathrm{e}^{\mathcal{D}[\sqrt{\Gamma}\hat{J}_-](t-t')}(\hat{J}_-\hat{X}(t')) \tag{E10}$$

$$= \sum_{m,m'=-m_0}^{j} Y_{m'm}|m'\rangle\langle m|, \tag{E11}$$

with $Y_{m'm} = 0$ for $m' = m - 1$. To complete the computation of the correlation function, we multiply by $\hat{J}_+$, defined by

$$\hat{J}_+ = \sum_{m=-m_0}^{m_0} \sqrt{m_0(m_0+1) - m(m-1)}\,|m\rangle\langle m-1|, \tag{E12}$$

and we obtain

$$\hat{J}_+\hat{Y} = \left(\sum_{m''=-m_0}^{m_0} \sqrt{m_0(m_0+1) - m''(m''-1)}\,|m''\rangle\langle m''-1|\right)\cdot \sum_{m,m'=-j}^{j} Y_{m'm}|m'\rangle\langle m|. \tag{E13}$$

We then take the trace of the above expression. Two delta functions appear: $\delta_{m''-1,m'}\delta_{m,m''}$, which give $m' = m - 1$. Since we had previously established that $Y_{m'm} = 0$, we conclude that the whole expression is zero. We thus found the result

$$\left.\frac{\partial g_1(t', t; \varphi)}{\partial \varphi}\right|_{\varphi=0} = 0, \tag{E14}$$

which means that time-integrated mode photon counting has zero linear sensitivity. Note that it is sufficient to show that the signal is zero to conclude that a linear estimator based on the mean photon number is not useful. If one wanted to compute the photon-number fluctuations as well, one would need to evaluate the four-time correlation function of the spin ensemble, too.

In Appendix K, we show that a photon-counting measurement saturates the quantum Fisher information if the arrival times of the photons are taken into account.

APPENDIX F: FLUCTUATIONS OF THE FILTERED INTEGRATED HOMODYNE CURRENT

We compute the fluctuations of the integrated current $\hat{M}_u$, which appear in the formula for the SNR in Eq. (22). We can write

$$\mathrm{Var}(\hat{M}_u) = \langle\hat{M}_u^2\rangle - \langle\hat{M}_u\rangle^2 = \int_0^\infty \mathrm{d}t' \int_0^\infty \mathrm{d}t\, S_{II,u}(t', t), \tag{F1}$$

with the correlation function defined in Eq. (23). We can break down the computation of this quantity by starting from the average of the observable, which is zero:

$$\langle\hat{M}_u\rangle = \int_0^\infty \mathrm{d}t\langle I_u(t)\rangle = 0, \tag{F2}$$

due to the fact that the expectation values of both $\hat{J}_+(t)$ and $\hat{J}_-(t)$ vanish under weak symmetry. When the state is omitted, the expectation value is assumed to be computed with respect to $|\Psi_0\rangle = |m_0\rangle \otimes |\Omega\rangle$. Consequently, we only need to compute $\langle\hat{M}_u^2\rangle$. We proceed by expressing it as a function of the current operator:

$$\begin{aligned}\langle\hat{M}_u^2\rangle &= \int_0^\infty \mathrm{d}t' \int_0^\infty \mathrm{d}t\langle\hat{I}_u(t')\hat{I}_u(t)\rangle \\ &= \int_0^\infty \mathrm{d}t' \int_0^\infty \mathrm{d}t\langle[u(t')\hat{b}_{\mathrm{out}}(t') + u^*(t')\hat{b}^\dagger_{\mathrm{out}}(t')] \\ &\quad\times [u(t)\hat{b}_{\mathrm{out}}(t) + u^*(t)\hat{b}^\dagger_{\mathrm{out}}(t)]\rangle.\end{aligned} \tag{F3}$$

Due to the rotational symmetry of the initial state, we can neglect the squeezing terms $\langle\hat{b}_{\mathrm{out}}(t')\hat{b}_{\mathrm{out}}(t)\rangle$ and $\langle\hat{b}^\dagger_{\mathrm{out}}(t')\hat{b}^\dagger_{\mathrm{out}}(t)\rangle$. We are then left with the expression:

$$\begin{aligned}\langle\hat{M}_u^2\rangle &= \int_0^\infty \mathrm{d}t' \int_0^\infty \mathrm{d}t\, u(t')u^*(t)\langle\hat{b}_{\mathrm{out}}(t')\hat{b}^\dagger_{\mathrm{out}}(t)\rangle \\ &\quad + \int_0^\infty \mathrm{d}t' \int_0^\infty \mathrm{d}t\, u^*(t')u(t)\langle\hat{b}^\dagger_{\mathrm{out}}(t')\hat{b}_{\mathrm{out}}(t)\rangle.\end{aligned} \tag{F4}$$

We observe that the integration domain over t' and t is symmetric under variable exchange. This implies that only

the component of the integrand that is symmetric in time contributes to the total integral. Thus, we can exchange the time variables $t' \leftrightarrow t$ in the second summand of Eq. (F4), yielding:

$$\langle \hat{M}_u^2 \rangle = \int_0^\infty \mathrm{d}t' \int_0^\infty \mathrm{d}t\, u(t')u^*(t)\langle \hat{b}_{\mathrm{out}}(t')\hat{b}_{\mathrm{out}}^\dagger(t)\rangle + \int_0^\infty \mathrm{d}t' \int_0^\infty \mathrm{d}t\, u^*(t)u(t')\langle \hat{b}_{\mathrm{out}}^\dagger(t)\hat{b}_{\mathrm{out}}(t')\rangle. \tag{F5}$$

By applying the commutation relations, we obtain the final formula for the fluctuations:

$$\begin{aligned}\langle \hat{M}_u^2 \rangle &= \int_0^\infty \mathrm{d}t' \int_0^\infty \mathrm{d}t\, u^*(t)[\delta(t-t') + 2\langle \hat{b}_{\mathrm{out}}^\dagger(t)\hat{b}_{\mathrm{out}}(t')\rangle]u(t') \\ &= \int_0^\infty \mathrm{d}t' \int_0^\infty \mathrm{d}t\, u^*(t)F(t,t')u(t') \\ &= \int_0^\infty \mathrm{d}t' \int_0^\infty \mathrm{d}t\, u^*(t')F(t',t)u(t),\end{aligned} \tag{F6}$$

where in the second-to-last step we have used the definition of the fluctuation function F, and in the final step we have exchanged the time variables via symmetrization.

There is also a second, more direct approach to the proof, which involves the introduction of the operator $\hat{N}_u \equiv \int_0^\infty \mathrm{d}t\, \hat{I}_u^\perp(t)$. This is the integral of the current operator $\hat{I}_u^\perp(t) = -i[u(t)\hat{b}_{\mathrm{out}}(t) - u^*(t)\hat{b}_{\mathrm{out}}^\dagger(t)]$, which corresponds to the quadrature orthogonal to $\hat{I}_u$. A direct computation using the commutation relations yields:

$$\langle \hat{M}_u^2 \rangle + \langle \hat{N}_u^2 \rangle = 2(2\bar{n}_u + 1), \tag{F7}$$

where $\bar{n}_u$ is the average photon number of the mode $u(t)$, as defined in Eq. (16). Due to the weak symmetry, the fluctuations of the two orthogonal quadratures are identical, i.e., $\langle \hat{M}_u^2 \rangle = \langle \hat{N}_u^2 \rangle$. This implies:

$$\langle \hat{M}_u^2 \rangle = \int_0^\infty \mathrm{d}t' \int_0^\infty \mathrm{d}t\, u^*(t')[2g_1(t',t) + \delta(t'-t)]u(t), \tag{F8}$$

which, by virtue of the definition in Eq. (15) for the two-point correlation function $g_1(t',t)$, gives the fluctuations as a function of F, noting that $F(t',t) = 2g_1(t',t) + \delta(t'-t)$.

APPENDIX G: ANALYTICAL COMPUTATION OF THE MAXIMUM SIGNAL-TO-NOISE RATIO MODE

In this appendix, we apply the Lagrange-multiplier formalism to optimize the SNR of the homodyne measurement, as it is defined in Eq. (25). The goal is to find the expression for the temporal mode $w_{\mathrm{SNR}}(t)$ reported in Eq. (26). We indicate by f the fluctuations of the mode $w_{\mathrm{SNR}}(t)$, computed according to Eq. (24):

$$f \equiv \int_0^\infty \mathrm{d}t' \int_0^\infty \mathrm{d}t\, w_{\mathrm{SNR}}^*(t')F(t',t)w_{\mathrm{SNR}}(t). \tag{G1}$$

We can reduce the minimization over $u(t)$ to the space of functions that have a fixed level of fluctuations f. We will see that we do not need to know the value of f to solve the optimization problem; we only need to assume that it exists. Let us write the Lagrangian for the maximization of the signal, given the fluctuations:

$$\mathcal{L}[u] \equiv 4\left|\mathrm{Re}\int_0^\infty \mathrm{d}t\, u(t)\alpha_I(t)\right|^2 - \lambda\left(\int_0^\infty \mathrm{d}t' \int_0^\infty \mathrm{d}t\, u^*(t')F(t',t)u(t) - f\right). \tag{G2}$$

The mode $w_{\mathrm{SNR}}(t)$ that maximizes the signal for fixed fluctuations is the solution to

$$\frac{\partial \mathcal{L}[u]}{\partial u^*(t)} = \alpha_I^*(t)\left(4\mathrm{Re}\int_0^\infty \mathrm{d}\tau\, u(\tau)\alpha_I(\tau)\right) - \lambda\int_0^\infty \mathrm{d}t'\, F(t,t')u(t') = 0. \tag{G3}$$

The scalar product $\int_0^\infty \mathrm{d}t\, u(t)\alpha_I(t)$ is a constant in time, albeit dependent on $u(t)$, so that we can write

$$u(t) \propto \int_0^\infty \mathrm{d}t'\, F^{-1}(t,t')\alpha_I^*(t'). \tag{G4}$$

After normalization, Eq. (G4) is the mode that optimizes the SNR.

An analytical expression for the maximum-SNR mode $w_{\mathrm{SNR}}(t)$ can be computed also when squeezing correlations are present in the state of the spins (and the emitted radiation), i.e., $\langle \hat{b}_{\mathrm{out}}(t')\hat{b}_{\mathrm{out}}(t)\rangle \neq 0$, by using the same Lagrange-multiplier formalism. This expression is never needed throughout the manuscript, but we nevertheless report a derivation of this optimized mode here. The Lagrangian with the fluctuations of the integrated homodyne current $\hat{I}_u$, for a mode $u(t)$, in the presence of squeezing correlations in the output field (originating from spin squeezing in the ensemble), can be written as

$$\begin{aligned}\mathcal{L}[u] \equiv 4&\left|\mathrm{Re}\int_0^\infty \mathrm{d}t\, u(t)\alpha_I(t)\right|^2 \\ &- \lambda\left(\int_0^\infty \mathrm{d}t' \int_0^\infty \mathrm{d}t\, u^*(t')F(t',t)u(t)\right. \\ &+ \int_0^\infty \mathrm{d}t' \int_0^\infty \mathrm{d}t\, u(t')B(t',t)u(t) \\ &\left.+ \int_0^\infty \mathrm{d}t' \int_0^\infty \mathrm{d}t\, u^*(t')B^\dagger(t',t)u^*(t) - f\right).\end{aligned} \tag{G5}$$

Here, $B(t',t) \equiv -\Gamma\langle \hat{J}_-(t')\hat{J}_-(t)\rangle$. We take the derivative with respect to $u^*(t)$ to find the optimal mode $u(t)$:

$$\frac{\partial \mathcal{L}[u]}{\partial u^*} = \alpha_I^*(t)\left(4\mathrm{Re}\int_0^\infty \mathrm{d}\tau\, u(\tau)\alpha_I(\tau)\right) \tag{G6}$$

$$-\lambda\int_0^\infty \mathrm{d}t'\, F(t,t')u(t') - \lambda\int_0^\infty \mathrm{d}t'\, B^\dagger(t,t')u^*(t') \tag{G7}$$

$$-\lambda\int_0^\infty \mathrm{d}t'\, B^*(t,t')u^*(t') = 0. \tag{G8}$$

We define $C \equiv 4\mathrm{Re}\int_0^\infty \mathrm{d}t\, u(t)\alpha_I(t) \in \mathbb{R}$. This equation for $u(t)$ can be solved by decomposing all the objects into real and imaginary parts, e.g., $F(t,t') = \mathrm{Re}F(t,t') + i\mathrm{Im}F(t,t')$, $B(t,t') = \mathrm{Re}B(t,t') + i\mathrm{Im}B(t,t')$, $u(t) = u_R(t) + iu_I(t)$, and $\alpha_I(t) = \mathrm{Re}\alpha_I(t) + i\mathrm{Im}\alpha_I(t)$, obtaining the following equations

$$\begin{aligned}
&-\mathrm{Im}\alpha_I - \mathrm{Im}F u_R - \mathrm{Re}F u_I + (\mathrm{Im}B)^\dagger u_R + (\mathrm{Re}B)^\dagger u_I \\
&\quad + (\mathrm{Im}B)^* u_R + (\mathrm{Re}B)^* u_I = 0, \\
&\mathrm{Re}\alpha_I - \mathrm{Re}F u_R + \mathrm{Im}F u_I - (\mathrm{Re}B)^\dagger u_R + (\mathrm{Im}B)^\dagger u_I \\
&\quad - (\mathrm{Re}B)^* u_R + (\mathrm{Im}B)^* u_I = 0,
\end{aligned} \tag{G9}$$

where we have simplified the notation for the integrals to a product, and we have absorbed λ and C into the definition of $u(t)$, which need not be normalized at this stage. This is a system of linear equations with two unknown functions $u_R(t)$ and $u_I(t)$, which we can write as follows

$$\begin{aligned}
&-\mathrm{Im}\alpha_I + [-\mathrm{Im}F + (\mathrm{Im}B)^\dagger + (\mathrm{Im}B)^*]u_R \\
&\quad + [-\mathrm{Re}F + (\mathrm{Re}B)^\dagger + (\mathrm{Re}B)^*]u_I = 0, \\
&\mathrm{Re}\alpha_I + [-\mathrm{Re}F - (\mathrm{Re}B)^\dagger - (\mathrm{Re}B)^*]u_R \\
&\quad + [\mathrm{Im}F + (\mathrm{Im}B)^\dagger + (\mathrm{Im}B)^*]u_I = 0.
\end{aligned} \tag{G10}$$

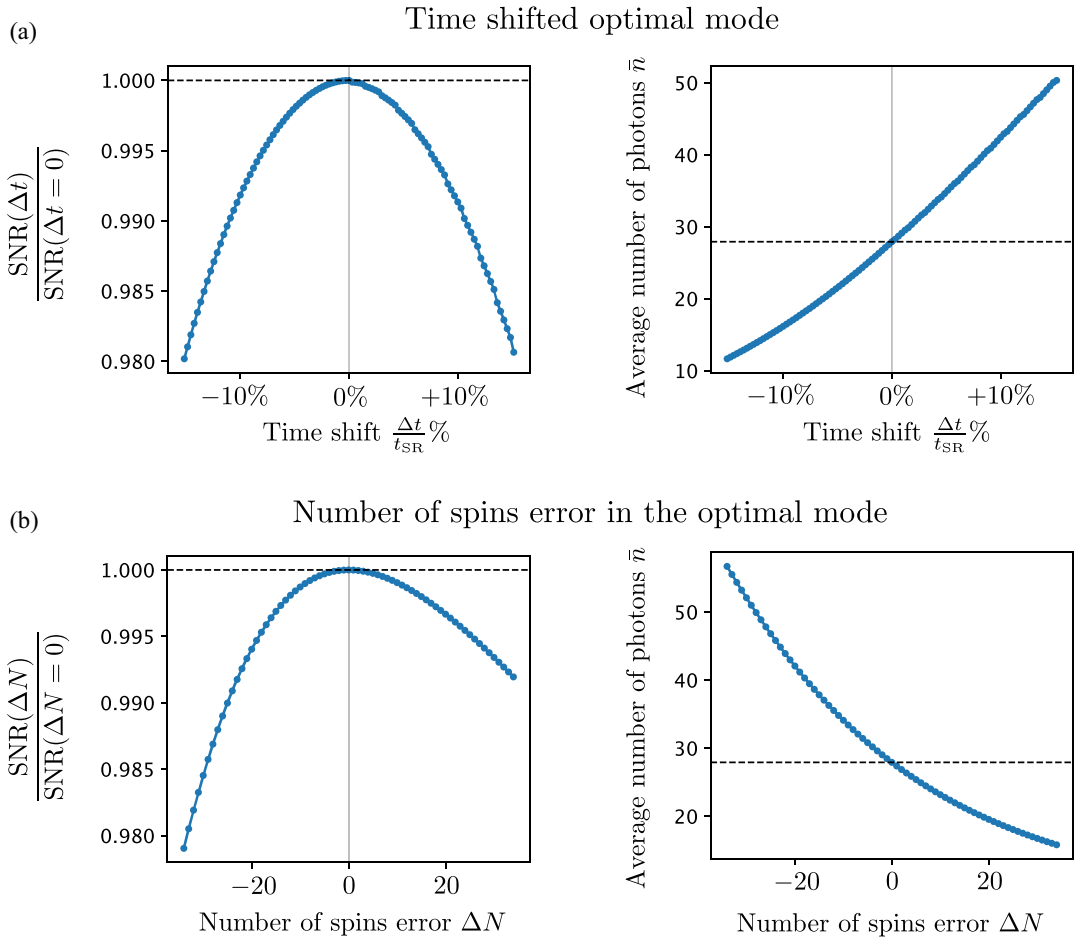


FIG. 5. Robustness of the optimized homodyne mode against representative mode mismatch. (a) The SNR and average photon number obtained when the optimal temporal mode is shifted by a time offset Δt. On the x axis we plot the time shift Δt as a percentage of the superradiant timescale t_{SR}. (b) The same quantities when the implemented temporal mode is computed for an assumed spin number $N + \Delta N$, but applied to a system with true spin number $N = 128$. The left plot shows the SNR normalized to its zero-mismatch value, while the right plot shows the absolute average photon number $\bar{n}$. Dashed lines indicate the unperturbed reference values.

We define

$$\begin{aligned} X_R &\equiv -\mathrm{Im}F + (\mathrm{Im}B)^\dagger + (\mathrm{Im}B)^*, \\ X_I &\equiv -\mathrm{Re}F + (\mathrm{Re}B)^\dagger + (\mathrm{Re}B)^*, \\ Z_R &\equiv -\mathrm{Re}F - (\mathrm{Re}B)^\dagger - (\mathrm{Re}B)^*, \\ Z_I &\equiv \mathrm{Im}F + (\mathrm{Im}B)^\dagger + (\mathrm{Im}B)^*, \end{aligned} \tag{G11}$$

and write the solution as

$$\begin{aligned} u_R &= (Z_R - Z_I X_I^{-1} X_R)^{-1}(-Z_I X_I^{-1}\mathrm{Im}\alpha_I - \mathrm{Re}\alpha_I), \\ u_I &= (Z_I - Z_R X_R^{-1} X_I)^{-1}(-Z_R X_R^{-1}\mathrm{Im}\alpha_I - \mathrm{Re}\alpha_I). \end{aligned} \tag{G12}$$

This concludes the derivation of the optimal mode.

APPENDIX H: ROBUSTNESS TO TEMPORAL-MODE MISMATCH

Here we provide representative numerical tests of the sensitivity of the optimized homodyne strategy to imperfections in the implemented temporal mode. We consider the resonant case and use the SNR-maximizing mode for $N = 128$ as the reference mode. In the first test, the implemented local-oscillator mode is shifted in time and then renormalized. The time shift is $\pm 10\%$ of the superradiant time-scale. In the second test, the implemented mode is the SNR-maximizing mode computed for a different assumed spin number, $N + \Delta N$.

The results are shown in Fig. 5. In both tests, the SNR remains within a few percent of its optimal value over the range shown. The average photon number in the implemented mode changes more strongly, but remains much smaller than N. These results indicate that the improvement associated with $w_{\mathrm{SNR}}(t)$ is not a fine-tuned consequence of an exactly implemented mode shape, but follows from a robust destructive-interference mechanism in the temporally correlated output field.

APPENDIX I: INTUITION FOR WHY THE MAX-SNR MODE HAS ALMOST NO PHOTONS IN IT

In this appendix, we discuss the interpretation of the maximum-SNR mode $w_{\mathrm{SNR}}(t)$, and how it can be informationally optimal while containing a vanishingly small fraction of the total photons. This section is not a derivation of the scaling law for the photon number in Fig. 4, and the results we derive rely heavily on assumptions that are not exactly satisfied by the superradiant system. Nevertheless, the toy models of this section clarify how it is plausible that the number of photons in $w_{\mathrm{SNR}}(t)$ scales sublinearly in the number of spins. We have not been able to find an analytical derivation of the scaling law that we empirically present in Fig. 4.

Generic conditions for having a max-SNR mode with almost no power and no signal. In Eq. (12), we have defined a homodyne current operator, from which we derive the signal $\alpha_I(t)$, and the mode of the output radiation which maximizes the signal, i.e., $w_{\mathrm{sig}}(t)$ defined in Eq. (21). A trivial, uncorrelated, white-noise background would imply that the best mode to filter in the homodyne detection is the (conjugated and normalized) signal mode itself. However, in our scenario, the nontrivial structure of the noise means that the optimal mode to measure is not simply the signal mode, as we see in Fig. 2.

To provide some intuition into the structure of the optimal max-SNR mode, we decompose it into a sum of two orthogonal terms: the first term involves the max-signal mode $w_{\mathrm{sig}}(t)$, while the second term involves an orthogonal normalized mode $z(t)$. For some $0 < s < 1$, we have:

$$w_{\mathrm{SNR}}(t) = \sqrt{1-s}\, w_{\mathrm{sig}}(t) + \sqrt{s}\, z(t). \tag{I1}$$

Note that any mode orthogonal to $w_{\mathrm{sig}}(t)$ has zero signal, so $z(t)$ has no signal (it is pure noise). See Fig. 6 for an example of a decomposition.

We now derive a formula for the coefficient s, which controls how much signal there is in the max-SNR mode. We denote the noise (the fluctuations of the homodyne current) of the signal mode $w_{\mathrm{sig}}(t)$ by f_w, while we denote by f_z the noise associated with $z(t)$. We write the covariance between these fluctuations as $\gamma\sqrt{f_w f_z}$, where $-1 \le \gamma \le 1$ is the correlation constant. The SNR can be written as a function of s, f_w, f_z and γ; up to a prefactor, it is

$$\mathrm{SNR} \propto \frac{1-s}{(1-s)f_w + s f_z + 2\gamma\sqrt{s(1-s)f_w f_z}}. \tag{I2}$$

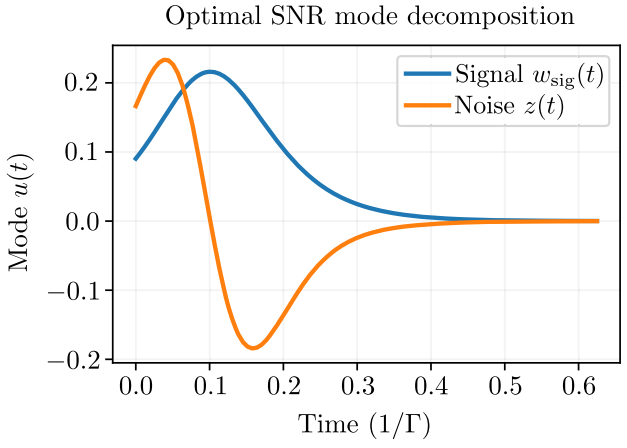


FIG. 6. Decomposition of the maximum SNR mode in Eq. (26) into a signal mode [Eq. (21)], and a zero-signal mode, for a small number $N = 16$.

By maximizing this expression over s, we get

$$\mathrm{SNR} \propto \frac{1}{f_w(1-\gamma^2)}. \tag{I3}$$

The optimal value of s^* is given by

$$s^* \equiv \frac{\gamma^2}{\frac{f_z}{f_w}+\gamma^2}. \tag{I4}$$

The above expression has an interesting limit that is of relevance to our system: when $f_z \ll f_w$ and the correlation constant γ is non-zero, the mode w_{SNR} becomes very close to the zero-signal mode $z(t)$, since s^* approaches one.

We can try to use these generic results to understand why in our superradiant setup the max-SNR mode has a vanishing fraction of the total photon number. We can do this by using the above expressions and making three mild assumptions:

1. The correlation constant γ tends to a non-zero constant in the large-N limit.
2. The signal mode fluctuations scale like N in the large-N limit, i.e., $f_w = \mathcal{O}(N)$.
3. The fluctuations in the no-signal mode $z(t)$ grow sublinearly with N in the large-N limit, implying $f_z/f_w \to 0$ for $N \to \infty$.

Note that point (2) above is rigorously true for our setup.

Given these conditions, the variance of the max-SNR mode reduces to:

$$f_{\mathrm{SNR}} \equiv \frac{\frac{f_z}{f_w}(1-\gamma^2)}{\frac{f_z}{f_w}+\gamma^2} f_w \simeq f_z \frac{1-\gamma^2}{\gamma^2}, \tag{I5}$$

where we have simplified $\frac{f_z}{f_w}$ because of assumption (3). Assumptions (2) and (3) now imply that the noise in the

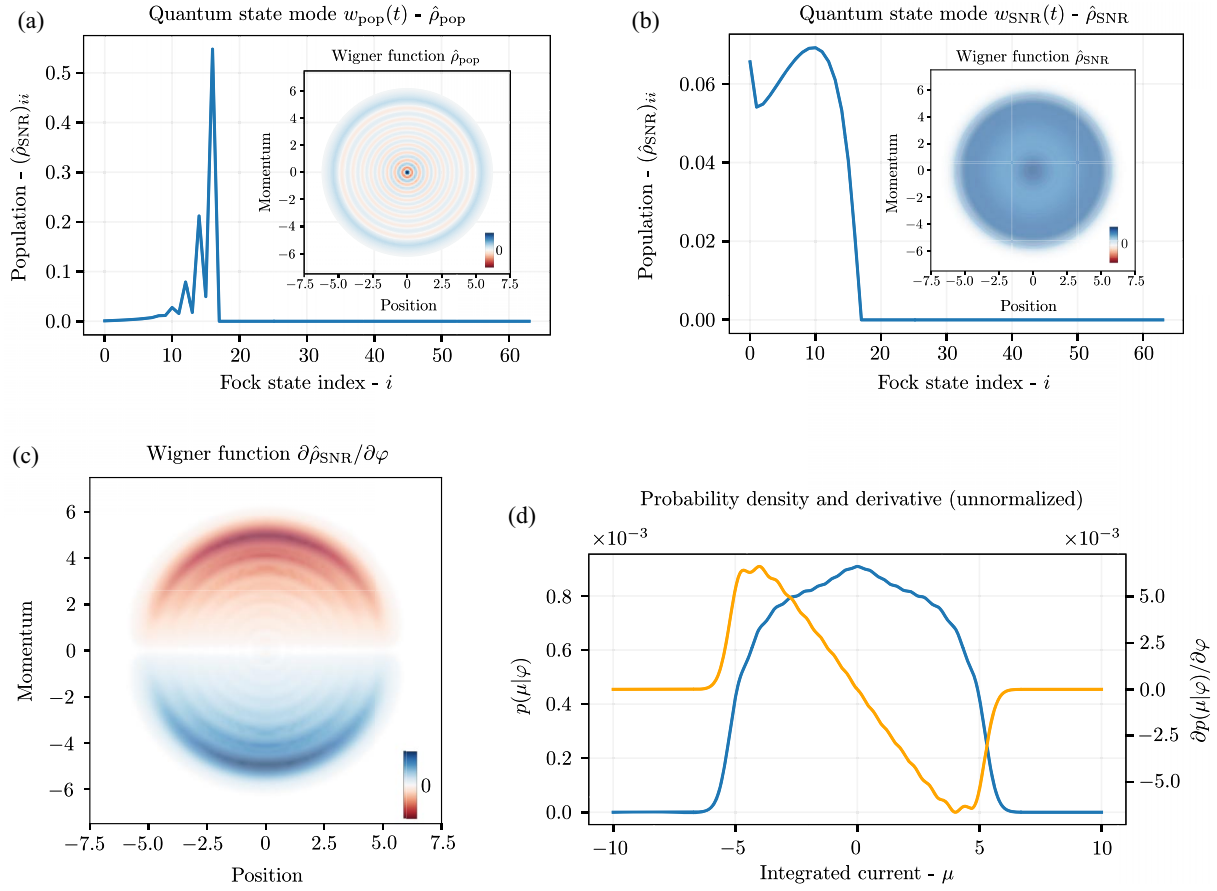


FIG. 7. (a) The picture represents the population of the most populated mode $w_{\mathrm{pop}}(t)$ for $N = 16$; the inset is its Wigner function; see Eq. (17). (b) Population and Wigner function of the mode that optimizes the SNR; see Eq. (26). Unlike $w_{\mathrm{pop}}(t)$, $w_{\mathrm{SNR}}(t)$ has no Wigner negativity. We observe that the uncertainty in the number of photons in the mode $w_{\mathrm{SNR}}(t)$ is larger than the uncertainty for the most populated mode. (c) Wigner function of the derivative of the state of the optimal mode (used to compute the QFI). (d) Probability density (and its derivative) of the integrated homodyne current. The density function is not normalized for better visualization in comparison with its derivative.

max-SNR mode will grow sublinearly with N, in the same manner as the noise f_z grows with N.

The upshot of this analysis is to provide an intuitive way of understanding how one could obtain a max-SNR mode that has almost no photons in it. We need the existence of a no-signal mode that has very few photons in it, but whose noise is correlated with the max-signal mode. In this case, the above optimization shows that the optimal strategy is to *primarily* measure the few-photon, no-signal mode, with just a tiny bit of the signal mode thrown in.

While this discussion provides some intuition, it of course leaves many things unanswered (e.g., why a low-photon-number, no-signal mode whose fluctuations are correlated with the max-signal mode exists).

APPENDIX J: COMPUTATION OF THE QUANTUM STATES

Computing nonlinear functions of the state of the radiation, like the Fisher information and the quantum Fisher information, requires the simulation of the state of the radiation itself [64]. This can be accomplished for a handful of modes through the cascaded master equation formalism [65–68].

In Fig. 7 we compare the states for the most populated mode in Eq. (17), called $\hat{\rho}_{\rm pop}$, and for the mode that maximizes the SNR in Eq. (26), called $\hat{\rho}_{\rm SNR}$. The fact that both these states are mixed is an indication of the entanglement between the modes. Because of the $U(1)$ symmetry we can say *a priori* that the density matrix of the quantum state of the light has zero off-diagonal elements.

From the mode state, we compute two information quantities that we compare with the QFI of the spin ensemble and with the SNR obtained from the homodyne measurement on the radiation. We compute the classical Fisher information associated with the measurement of the integrated homodyne current, i.e., the measurement of the observable $\hat{M}_u$ in Eq. (19). We denote this measurement-dependent CFI by $F_\varphi(\hat{M}_u)$, reserving $\mathcal{F}_\varphi(\hat{\rho})$ for the QFI of a state $\hat{\rho}$. This precision is achievable with an optimized estimator that goes beyond Eq. (D7). The second information quantity we compute is the QFI of the mode, which is the ultimate precision limit in the estimation of φ associated with the most general measurement on the reduced state of the mode only. We evaluate these quantities for the encoding of the rotation angle in Eq. (5), where the QFI of the spin ensemble is the standard quantum limit, i.e., $\mathcal{F}_\varphi(|\psi_\varphi^S\rangle) = N$, for small values of the number of spins N. We report these results in Table II. This table shows that, even if we were able to extract the full QFI from the state of the mode $\hat{\rho}_{\rm SNR}$, the improvement over the linear estimation would be marginal. This is because the mode in Eq. (26) is optimized to maximize the SNR and not the QFI. We cannot exclude the existence of a QFI-optimal mode that achieves the full QFI of the spin ensemble. The computation of these modes, which we think can only be done numerically, goes beyond the scope of this paper.

TABLE II. QFI and CFI for the mode $w_{\rm SNR}(t)$ in Eq. (26), for small values of the number of spins in the ensemble. These information quantities are to be compared with the SNR achievable by the linear estimator; see Fig. 2.

Num. spins (N)	$\mathcal{F}_\varphi(\hat{\rho}_{\rm SNR})/N$	$F_\varphi(\hat{M}_{w_{\rm SNR}})/N$
4	0.77	0.53
8	0.54	0.45
16	0.47	0.46

APPENDIX K: OPTIMALITY OF THE HOMODYNE AND PHOTON COUNTING MEASUREMENTS

In this appendix, we prove the optimality of homodyne detection and photon counting for the estimation of the rotation angle imprinted on the initial state of the spin ensemble in Eq. (5). This proof is valid if the cavity is exactly on resonance with the spin ensemble, and if the spins are initially fully excited. This result concerns the full time-resolved measurement record, not the single-mode linear estimator analyzed in the main text. For photon counting, it assumes access to photon arrival times with arbitrarily fine time resolution. The proof first maps the initial-value problem to an equivalent continuous-encoding description in which the parameter appears in the collective jump operator and then applies the Fisher-information conditions of Ref. [34] to the resulting continuous-measurement trajectories.

First, we observe that the state of light emitted by a spin ensemble whose initial state encodes the parameter φ is identical to that emitted by an initially fully polarized ensemble subject to φ-dependent dissipation. This mapping, which is itself a novel result concerning the dynamics of a decaying spin ensemble, connects the initial encoding to a continuous-encoding problem. We can then prove that time-resolved measurements saturate the QFI of the spin ensemble using techniques analogous to those of Ref. [34]. That work studies a Hamiltonian encoding of the parameter, whereas we consider dissipative encoding.

1. Mapping to a dissipative continuous-encoding problem

Equivalence with a continuous encoding problem. Recently, there has been progress in the effort to define the maximum achievable precision in the estimation of continuously encoded parameters, together with the effort to find the measurement that achieves this maximum [64,69,70]. We show in this section how the initial-value

problem codified by Eq. (5) can be transformed into a continuous encoding scenario with a dissipator that depends on φ, the parameter to be estimated. This allows us to exploit the results of Ref. [34] and to prove that the Fisher information of the continuous measurements (photon counting and homodyne detection) achieves exactly the quantum Fisher information in Eq. (4). The estimator for φ, needed to saturate the QFI, involves in principle all complex higher-order temporal correlation functions of the homodyne current. This proof does not extend to the case where there is detuning between the cavity and the spins, or to the use of twist-untwist encoding. Therefore, it does not extend to the achievability of the Heisenberg scaling. It is surprising that the QFI of the entangled and multimodal state of the light is exactly achievable with local measurements on the output field.

New reference frame for the spin ensemble. In the following, we give an equivalent description of the state of the light emitted by the spins in superradiance, which is based on a continuous encoding scenario instead of the initial-value problem. We denote by $\hat{\rho}_\varphi$ the pure state in Eq. (5). At time $t = 0$ the initial state of the spin ensemble and the waveguide is $\hat{\rho}_\varphi \otimes |0\rangle\langle 0|$, with the waveguide being in the vacuum state. We call $\hat{U}_{SR}^{(0\to t)}$ the joint unitary evolution of the ensemble of spins and the infinitely many modes of the waveguide, such that we can write the state of the radiation field at time t by tracing out the spins:

$$\hat{\rho}_R^{\varphi}(t) \equiv \mathrm{Tr}_S\left[\hat{U}_{SR}^{(0\to t)}(\hat{\rho}_\varphi \otimes |0\rangle\langle 0|)\hat{U}_{SR}^{(0\to t)\dagger}\right]. \tag{K1}$$

We apply a change of reference frame for the ensemble of spins by acting with the inverse of the unitary in Eq. (5), which is just a rotation around the y axis that undoes the encoding of the spins:

$$\hat{\rho}_R^{\varphi}(t) \equiv \mathrm{Tr}_S\Big[\hat{U}_{-\varphi}\hat{U}_{SR}^{(0\to t)}\hat{U}_{-\varphi}^{\dagger}\hat{U}_{-\varphi}(\hat{\rho}_\varphi \otimes |0\rangle\langle 0|) \times \hat{U}_{-\varphi}^{\dagger}\hat{U}_{-\varphi}\hat{U}_{SR}^{\dagger(0\to t)}\hat{U}_{-\varphi}^{\dagger}\Big]. \tag{K2}$$

Inserting the unitary $\hat{U}_{-\varphi}$, which is acting only on the spins, leaves the trace unchanged. The joint initial state of the spins and the waveguide becomes independent of φ in the new frame:

$$\hat{U}_{-\varphi}(\hat{\rho}_\varphi \otimes |0\rangle\langle 0|)\hat{U}_{-\varphi}^{\dagger} = \hat{\rho} \otimes |0\rangle\langle 0|, \tag{K3}$$

where $\hat{\rho} \equiv |m_0\rangle\langle m_0|$ is the fully excited state of the spins.

As for the action of the change of reference on the interaction unitary $\hat{U}_{SR}^{(0\to t)}$, we can start from the explicit definition of $\hat{U}_{SR}^{(0\to t)}$, which involves the spins and the radiation modes of the waveguide while the cavity has been adiabatically eliminated. The definition of this unitary is

$$\hat{U}_{SR}^{(0\to t)} = \exp\Big[-i\Big(\hat{H}_R + \hat{H}_S + \sum_k (g_k\hat{J}_+\hat{b}_k + g_k^*\hat{J}_-\hat{b}_k^\dagger)\Big)t\Big], \tag{K4}$$

where $\hat{H}_R$ is the free Hamiltonian of the radiation, $\hat{H}_S$ is the Hamiltonian of the spins, and the interaction term features the lowering and raising operators of the spin ensemble coupled to the bosonic operators of the waveguide modes in the momentum basis, $\hat{b}_k$ and $\hat{b}_k^\dagger$. The action of $\hat{U}_{-\varphi}$ leaves $\hat{H}_R$ unchanged, while the free Hamiltonian of the spins becomes $\hat{H}_S \to \hat{U}_{-\varphi}\hat{H}_S\hat{U}_{-\varphi}^\dagger$. Similarly, the angular momentum operators in the interaction term become $\hat{J}_- \to \hat{U}_{-\varphi}\hat{J}_-\hat{U}_{-\varphi}^\dagger$ and $\hat{J}_+ \to \hat{U}_{-\varphi}\hat{J}_+\hat{U}_{-\varphi}^\dagger$. We now define the unitary operator for the superradiant evolution in the new reference frame as

$$\hat{U}_{SR,\varphi}^{(0\to t)} \equiv \hat{U}_{-\varphi}\hat{U}_{SR}^{(0\to t)}\hat{U}_{-\varphi}^\dagger, \tag{K5}$$

so that the state of the light at time t is described by tracing out the spins subject to the φ-dependent evolution $\hat{U}_{SR,\varphi}^{(0\to t)}$, i.e.,

$$\hat{\rho}_R^{\varphi}(t) = \mathrm{Tr}_S\left[\hat{U}_{SR,\varphi}^{(0\to t)}(\hat{\rho} \otimes |0\rangle\langle 0|)\hat{U}_{SR,\varphi}^{(0\to t)\dagger}\right]. \tag{K6}$$

In order to describe the reduced dynamics of the spins only, we can trace out the degrees of freedom of the radiation field to obtain the master equation for the spins. For the Hamiltonian part we can assume $\hat{H}_S = 0$, i.e., we choose the original frame of reference to be rotating with the frequency of the spins. Starting from Eq. (K5), we write explicitly the form of the interaction $\hat{U}_{SR,\varphi}^{(0\to t)}$ as

$$\hat{U}_{SR,\varphi}^{(0\to t)} = \exp\Big[-i\Big(\hat{H}_R + \sum_k (g_k\hat{U}_{-\varphi}\hat{J}_+\hat{U}_{-\varphi}^\dagger\hat{b}_k + g_k^*\hat{U}_{-\varphi}\hat{J}_-\hat{U}_{-\varphi}^\dagger\hat{b}_k^\dagger)\Big)t\Big]. \tag{K7}$$

Comparing this expression with Eq. (K4), we see that the superradiant decay of the ensemble can be described by the superoperator $\mathcal{D}[\hat{U}_{-\varphi}\hat{J}_-\hat{U}_{-\varphi}^\dagger]$. To be explicit, in the new frame, the dynamics of the spin ensemble is described by the φ-dependent Lindbladian:

$$\partial_t\hat{\rho}(t) = \Gamma\mathcal{D}[\hat{U}_{-\varphi}\hat{J}_-\hat{U}_{-\varphi}^\dagger]\hat{\rho}(t). \tag{K8}$$

This describes a superradiant decay process along an axis tilted from z by an angle φ. At the same time, the initial state of the spins is $\hat{\rho}(0) \equiv |m_0\rangle\langle m_0|$.

A related mapping was established in Ref. [22]: a unitary parameter encoding imposed by linear-optical

elements on the output field of a general Markovian light source, including a superradiant source, can be represented by parameter-dependent source jump operators.

Note that a byproduct of this transformation is an alternate, but equivalent way to look at the main results of our work. It also describes the measurement physics of a particular class of continuous metrology setups where the parameter of interest modulates a collective spin dissipator. Our results are also striking in this setting: we show a simple way of achieving Heisenberg-limited scaling in N using a simple homodyne measurement of the output field. This should be contrasted against schemes where achieving optimal scaling requires a second physical system to process the output field before measurement, e.g., a coherent quantum absorber [71,72].

2. Fisher information of the full measurement record

Information analysis of the continuous encoding scenario. In the previous paragraphs, we have constructed a conceptually different encoding process for the rotation angle φ, which gives us an alternative and completely equivalent way to compute the state of the light during the superradiant decay. We define two scenarios, called scenario I and scenario II. The first one is an initial-value problem, where the rotation angle is encoded in the initial state of the spin ensemble, and the decay operator on the spins is $\mathcal{D}[\hat{J}_-]$. This is the scenario of the main text. Scenario II is a continuous encoding scheme, where the decay operator is $\mathcal{D}[\hat{U}_{-\varphi}\hat{J}_-\hat{U}^\dagger_{-\varphi}]$, and was introduced above. We are interested in working in the limit $t\to\infty$, where the state of the radiation and the spins is separable. While the state of the radiation is the same in both scenarios, the state of the spins is different. In scenario I, the spins are in the lower energy state $|-m_0\rangle$, while in scenario II, the final state of the spins is the rotated state $\hat{U}_{-\varphi}|-m_0\rangle$. This makes a difference for the computation of the total asymptotic quantum Fisher information of the joint system. In scenario I, the spins have no information on φ because their state is completely decayed, while the radiation contains the full quantum Fisher information of the initial state of the ensemble of spins, i.e., $\mathcal{F}_\varphi(\hat{\rho}^\varphi_R(t\to\infty))=N$. If we consider instead scenario II, we find that the spins have been encoded with the parameter φ, so that the final QFI is $\mathcal{F}_\varphi(\hat{U}_{-\varphi}|-m_0\rangle)+\mathcal{F}_\varphi(\hat{\rho}^\varphi_R(t\to\infty))=2N$, i.e., twice that of scenario I. This also underlines how these two scenarios are not equivalent in terms of the metrological analysis; only the state of the light produced is the same.

Continuous measurements. We now consider the use of continuous measurements, measuring the radiation as it is generated by the decaying spins. We use the term *trajectory* to indicate the full list of observed results of the continuous measurement. We denote by $F^{h,c}(p_{\text{traj}})$ the classical Fisher information we can extract from the full trajectory of outcomes from these measurements, where p_{traj} is the probability distribution for the trajectories. We use the notation F^c for the CFI of photon counting, while F^h is the CFI of homodyne detection.

In general, after the continuous measurement, the spin ensemble will be in a conditional state that depends on the trajectory, which we denote by $\hat{\rho}^{\text{traj}}_\varphi$. A final measurement is performed on this state of the spins, with the optimal measurement saturating the QFI. From Ref. [25], we write the total Fisher information extracted from the continuous measurement as

$$F^{h,c}=F^{h,c}(p_{\text{traj}})+\mathbb{E}_{\text{traj}}[\mathcal{F}_\varphi(\hat{\rho}^{\text{traj}}_\varphi)]. \tag{K9}$$

In scenario I (initial-value encoding), the final state of the spins long after the decay is independent of the trajectory and of φ, so that we have

$$F^{h,c}_I=F^{h,c}_I(p_{\text{traj}}). \tag{K10}$$

In scenario II (continuous encoding), the final state of the spins is also independent of the trajectory, and we have

$$F^{h,c}_{II}=F^{h,c}_{II}(p_{\text{traj}})+\mathcal{F}_\varphi(\hat{U}_{-\varphi}|-m_0\rangle) \tag{K11}$$

$$=F^{h,c}(p_{\text{traj}})+N. \tag{K12}$$

We will prove in the next paragraph that homodyne detection and photon counting both saturate the joint QFI of the spins and the radiation field, so that we can write $F^{h,c}_{II}(p_{\text{traj}})+N=2N$, which implies $F^{h,c}_{II}(p_{\text{traj}})=N$. The final observation to connect this result to scenario I is that $F^{h,c}_{II}(p_{\text{traj}})$ depends only on the state of the radiation, which is the same in scenarios I and II, which implies $F^{h,c}_I(p_{\text{traj}})=F^{h,c}_{II}(p_{\text{traj}})$, so that we have

$$F^{h,c}_I(p_{\text{traj}})=\mathcal{F}_\varphi(|\psi^S_\varphi\rangle), \tag{K13}$$

since $\mathcal{F}_\varphi(|\psi^S_\varphi\rangle)=N$. The continuous measurement on the state of the radiation field is sufficient to achieve the QFI in the initial-value problem, when the full statistics deriving from the outcome trajectories are accounted for. In the rest of this section, we prove that the continuous measurements in scenario II are optimal. We start by computing a simple formula for the global QFI of the spins and the radiation field, and we conclude by proving that $F^{c,h}_{II}$ achieves it for both measurements.

Continuous measurements from a collisional model. Within a collisional model description of the environment of the spins [73], we compute the joint evolution of the system and the environment by discretizing time into small steps Δt, and introducing a new instance of the Hilbert space of a single mode of the radiation field for each time step. The same reduced dynamics on the system of spins

can be described by different Kraus operators according to the continuous measurement performed on the radiation modes (photon counting or homodyne detection). The outcome of the measurement on the environment at each time step is i_j, with j being the index of the time step. These outcomes are also the indices of the Kraus operators for each instantaneous measurement, and each can take a continuous value, i.e., $J_j \equiv i_j \in \mathbb{R}$, or a binary value, i.e., $i_j \in \{0, 1\}$. We now define the Kraus operators for photon counting and homodyne detection, for a single time step, so that we can suppress the subscript j for simplicity. Let us define the rotated jump operator $\hat{L}_\varphi \equiv \sqrt{\Gamma}\hat{U}_{-\varphi}\hat{J}_-\hat{U}^\dagger_{-\varphi}$. Then the Kraus operators corresponding to photon counting in scenario II are

$$\hat{K}^\varphi_0 \equiv e^{-\frac{1}{2}\hat{L}^\dagger_\varphi \hat{L}_\varphi \Delta t}, \qquad \hat{K}^\varphi_1 \equiv \sqrt{\Delta t}\hat{L}_\varphi. \tag{K14}$$

These two operators correspond to no photon detected ($\hat{K}^\varphi_0$), and a single photon collected ($\hat{K}^\varphi_1$). The Kraus operators satisfy $\hat{K}^{\varphi\dagger}_0\hat{K}^\varphi_0 + \hat{K}^{\varphi\dagger}_1\hat{K}^\varphi_1 = \mathbb{1}$ to leading order in Δt. We now discuss the form of the Kraus operators for homodyne detection. In order to describe homodyne detection on the quadrature $\hat{L}_\varphi e^{i\theta} + \hat{L}^\dagger_\varphi e^{-i\theta}$, we need a continuous set of Kraus operators, indexed by the value of the homodyne current measured at each time step, i.e.

$$\hat{K}^\varphi_J \equiv 1 - \frac{\hat{L}^\dagger_\varphi \hat{L}_\varphi}{2}\Delta t + \hat{L}_\varphi e^{i\theta} J \Delta t. \tag{K15}$$

We introduce the normalized Gaussian ostensive probability density $q_{\Delta t}(J) \equiv \sqrt{\Delta t/(2\pi)}\exp(-\Delta t J^2/2)$, which is needed to normalize the continuous-outcome Kraus operators properly [74]. The Kraus operators for homodyne detection then satisfy

$$\int_{-\infty}^{+\infty} \mathrm{d}J\, q_{\Delta t}(J)\hat{K}^{\varphi\dagger}_J \hat{K}^\varphi_J = \mathbb{1} + \mathcal{O}(\Delta t^2). \tag{K16}$$

In this section, unless otherwise specified, we will always assume $\theta = 0$. We denote by $(i_j)_{j=1}^M$ the tuple containing the full set of outcomes, i.e., the trajectory. Given a certain trajectory, the unnormalized state of the ensemble of spins is

$$|\tilde{\psi}_{\mathrm{traj}}(\varphi)\rangle \equiv \hat{K}^\varphi_{i_M}\hat{K}^\varphi_{i_{M-1}}\cdots\hat{K}^\varphi_{i_2}\hat{K}^\varphi_{i_1}|\psi\rangle. \tag{K17}$$

The state of the copy of the environment at the time step j is $|i_j\rangle$, so that $|i_1, \cdots, i_M\rangle$ is the full state of the environment. Summing over all possible trajectories gives the full entangled state of the spins and the radiation:

$$|\Psi_\varphi(t)\rangle \equiv \sum_{(i_j)_{j=1}^M} \hat{K}^\varphi_{i_M}\hat{K}^\varphi_{i_{M-1}}\cdots\hat{K}^\varphi_{i_2}\hat{K}^\varphi_{i_1}|\psi\rangle \otimes |i_1, \cdots, i_M\rangle. \tag{K18}$$

Expression for the joint QFI. The quantum Fisher information of the joint state $|\Psi_\varphi(t)\rangle$ is

$$\mathcal{F}_\varphi(|\Psi_\varphi(t)\rangle) = 4(\langle\partial_\varphi\Psi_\varphi(t)|\partial_\varphi\Psi_\varphi(t)\rangle - |\langle\Psi_\varphi(t)|\partial_\varphi\Psi_\varphi(t)\rangle|^2), \tag{K19}$$

where we have used the notation $|\partial_\varphi\Psi_\varphi(t)\rangle \equiv \partial|\Psi_\varphi(t)\rangle/\partial\varphi$. We first write the expression for $|\partial_\varphi\Psi_\varphi(t)\rangle$ in terms of the Kraus operators

$$|\partial_\varphi\Psi_\varphi(t)\rangle = \sum_{j=1}^M \sum_{(i_l)_{l=1}^M} \hat{K}^\varphi_{i_M}\hat{K}^\varphi_{i_{M-1}}\cdots\hat{K}^\varphi_{i_{j+1}}\left(\partial_\varphi\hat{K}^\varphi_{i_j}\right) \times \hat{K}^\varphi_{i_{j-1}}\cdots\hat{K}^\varphi_{i_1}|\psi\rangle \otimes |i_1, i_2, \cdots, i_M\rangle \tag{K20}$$

$$= \sum_{(i_l)_{l=1}^M} \sum_{j=1}^M \hat{K}^\varphi_{i_M}\hat{K}^\varphi_{i_{M-1}}\cdots\hat{K}^\varphi_{i_{j+1}}\left(\partial_\varphi\hat{K}^\varphi_{i_j}\right) \times \hat{K}^\varphi_{i_{j-1}}\cdots\hat{K}^\varphi_{i_1}|\psi\rangle \otimes |i_1, i_2, \cdots, i_M\rangle, \tag{K21}$$

where in the second equation we have swapped the summations. We can compute the norm of the derivative $|\partial_\varphi\Psi_\varphi(t)\rangle$ by observing that states of the environment corresponding to different trajectories are orthogonal to each other, so that the total norm of the derivative is the sum of the norms of the derivatives of the unnormalized states of the spins:

$$\langle\partial_\varphi\Psi_\varphi(t)|\partial_\varphi\Psi_\varphi(t)\rangle \times \sum_{(i_l)_{l=1}^M} \left\| \sum_{j=1}^M \hat{K}^\varphi_{i_M}\cdots\hat{K}^\varphi_{i_{j+1}}\left(\partial_\varphi\hat{K}^\varphi_{i_j}\right)\hat{K}^\varphi_{i_{j-1}}\cdots\hat{K}^\varphi_{i_1}|\psi\rangle \right\|^2. \tag{K22}$$

We now consider the second term of the QFI in Eq. (K19), and we write explicitly the expression for the scalar product of $|\Psi_\varphi(t)\rangle$ and its derivative, by introducing the Kraus operators and the summation over the trajectories:

$$\langle\Psi_\varphi(t)|\partial_\varphi\Psi_\varphi(t)\rangle = \sum_{j=1}^M \sum_{(i_l)_{l=1}^j} \langle\psi|\hat{K}^{\varphi\dagger}_{i_1}\cdots\hat{K}^{\varphi\dagger}_{i_{j-1}}\hat{K}^{\varphi\dagger}_{i_j} \times \left(\partial_\varphi\hat{K}^\varphi_{i_j}\right)\hat{K}^\varphi_{i_{j-1}}\cdots\hat{K}^\varphi_{i_1}|\psi\rangle. \tag{K23}$$

We will prove in the next paragraphs that this term is zero, both for homodyne detection and for photon counting, so that we can simplify the expression for the QFI to

the term in Eq. (K22) only. The state of the environment and the spins at a certain time is independent of the choice of the measurement; therefore, we need to prove the statement for only one of photon counting and homodyne detection. That is, both unravellings of the dynamics with different Kraus operators must give the same results for $|\Psi_\varphi(t)\rangle$ and its derivatives. Nevertheless, in the following, we report both proofs in order to introduce the two different expressions for the Fisher information for the two different continuous measurements.

Joint QFI of the spins and the radiation for photon counting. We commute the summations over the time index and over the trajectories and write two separate families of trajectories, according to the value of i_j:

$$\begin{aligned}&\langle\Psi_\varphi(t)|\partial_\varphi\Psi_\varphi(t)\rangle\\&=\sum_{j=1}^{M}\sum_{\substack{(i_l)_{l=1}^{j}\\ i_j=0}}\langle\psi|\hat{K}_{i_1}^{\varphi\dagger}\cdots\hat{K}_0^{\varphi\dagger}\left(\partial_\varphi\hat{K}_0^{\varphi}\right)\cdots\hat{K}_{i_1}^{\varphi}|\psi\rangle\\&\quad+\sum_{j=1}^{M}\sum_{\substack{(i_l)_{l=1}^{j}\\ i_j=1}}\langle\psi|\hat{K}_{i_1}^{\varphi\dagger}\cdots\hat{K}_1^{\varphi\dagger}\left(\partial_\varphi\hat{K}_1^{\varphi}\right)\cdots\hat{K}_{i_1}^{\varphi}|\psi\rangle.\end{aligned}\tag{K24}$$

We write explicitly the term

$$\begin{aligned}\hat{L}_\varphi^\dagger\hat{L}_\varphi&=\Gamma\hat{U}_{-\varphi}\hat{J}_+\hat{J}_-\hat{U}_{-\varphi}^\dagger\\&=\Gamma\left(m_0(m_0+1)-\hat{U}_{-\varphi}\hat{J}_z^2\hat{U}_{-\varphi}^\dagger+\hat{U}_{-\varphi}\hat{J}_z\hat{U}_{-\varphi}^\dagger\right).\end{aligned}\tag{K25}$$

This lets us compute the derivative

$$\begin{aligned}\hat{K}_0^{\varphi\dagger}\partial_\varphi\hat{K}_0^{\varphi}|_{\varphi=0}&=-\frac{i}{2}\Gamma\Delta t[\hat{J}_y,\hat{J}_z^2-\hat{J}_z]\\&=\frac{\Gamma\Delta t}{2}\left(\{\hat{J}_x,\hat{J}_z\}-\hat{J}_x\right)+\mathcal{O}(\Delta t^2).\end{aligned}\tag{K26}$$

The first summand of Eq. (K24) is proportional to the expectation value of the operator $\{\hat{J}_x,\hat{J}_z\}-\hat{J}_x$ evaluated on the unnormalized state of the spins evolved up to time $t=j\Delta t$, summed over all possible trajectories. Because of the sum over all trajectories, we can turn this term into the weighted expectation value over the normalized state conditioned on the trajectory, which is simply the expectation value over the reduced state of the spins. In other words, the first summand evaluates to the integral of $\langle\{\hat{J}_x(t),\hat{J}_z(t)\}-\hat{J}_x(t)\rangle$, where $\hat{J}_x(t)$ and $\hat{J}_z(t)$ are the spin operators in the Heisenberg representation and the expectation value is computed over the initial state of the spins $|m_0\rangle$. It can be verified numerically that this expectation value is identically zero, because of the rotational symmetry of the initial state around the z axis. We now focus on the second summand of Eq. (K24). We write the innermost product as

$$\hat{K}_1^{\varphi\dagger}\partial_\varphi\hat{K}_1^{\varphi}\propto\hat{J}_+[\hat{J}_y,\hat{J}_-]=\hat{J}_+[\hat{J}_y,\hat{J}_x]\propto\hat{J}_+\hat{J}_z,\tag{K27}$$

which, because of rotational symmetry, also has zero expectation value. We conclude that the expression in Eq. (K24) is identically zero, i.e., $\langle\Psi_\varphi(t)|\partial_\varphi\Psi_\varphi(t)\rangle=0$. We finally write the expression for the total QFI of the joint system of spins and radiation, valid for every time t:

$$\begin{aligned}&\mathcal{F}_\varphi(|\Psi_\varphi(t)\rangle)\\&=4\langle\partial_\varphi\Psi_\varphi(t)|\partial_\varphi\Psi_\varphi(t)\rangle\\&=4\sum_{(i_j)_{j=1}^{M}}\left\|\sum_{j=1}^{M}\hat{K}_{i_M}^{\varphi}\cdots\hat{K}_{i_{j+1}}^{\varphi}\left(\partial_\varphi\hat{K}_{i_j}^{\varphi}\right)\hat{K}_{i_{j-1}}^{\varphi}\cdots\hat{K}_{i_1}^{\varphi}|\psi\rangle\right\|^2.\end{aligned}\tag{K28}$$

Joint QFI of the spins and the radiation for homodyne detection. Because of the different normalization of the Kraus operators for homodyne detection, the joint state of the ensemble of spins and the radiation is written as

$$\begin{aligned}|\Psi(t)\rangle=&\int_{-\infty}^{+\infty}\mathrm{d}J_M\,\sqrt{q_{\Delta t}(J_M)}\cdots\\&\times\int_{-\infty}^{+\infty}\mathrm{d}J_1\,\sqrt{q_{\Delta t}(J_1)}\\&\cdot\hat{K}_{J_M}^{\varphi}\hat{K}_{J_{M-1}}^{\varphi}\cdots\hat{K}_{J_j}^{\varphi}\cdots\hat{K}_{J_1}^{\varphi}|\psi\rangle\\&\otimes|J_1,J_2,\cdots,J_M\rangle.\end{aligned}\tag{K29}$$

We evaluate the derivative of this state as a function of the parameter φ:

$$\begin{aligned}|\partial_\varphi\Psi(t)\rangle=&\sum_{j=1}^{M}\int_{-\infty}^{+\infty}\mathrm{d}J_M\,\sqrt{q_{\Delta t}(J_M)}\cdots\\&\times\int_{-\infty}^{+\infty}\mathrm{d}J_1\,\sqrt{q_{\Delta t}(J_1)}\\&\cdot\hat{K}_{J_M}^{\varphi}\cdots(\partial_\varphi\hat{K}_{J_j}^{\varphi})\cdots\hat{K}_{J_1}^{\varphi}|\psi\rangle\\&\otimes|J_1,\cdots,J_M\rangle.\end{aligned}\tag{K30}$$

As in the photon counting case, we write

$$\begin{aligned}\langle\Psi(t)|\partial_\varphi\Psi(t)\rangle=&\sum_{j=1}^{M}\int_{-\infty}^{+\infty}\mathrm{d}J_M\,q_{\Delta t}(J_M)\cdots\\&\times\int_{-\infty}^{+\infty}\mathrm{d}J_1\,q_{\Delta t}(J_1)\\&\times\langle\psi|\hat{K}_{J_1}^{\varphi\dagger}\cdots\hat{K}_{J_j}^{\varphi\dagger}(\partial_\varphi\hat{K}_{J_j}^{\varphi})\cdots\hat{K}_{J_1}^{\varphi}|\psi\rangle.\end{aligned}\tag{K31}$$

We next average the innermost product over this Gaussian weight. Using $\int\mathrm{d}J\,q_{\Delta t}(J)J=0$ and

$\int \mathrm{d}J\, q_{\Delta t}(J) J^2 = 1/\Delta t$, we obtain

$$\begin{aligned}
&\int_{-\infty}^{+\infty} \mathrm{d}J\, q_{\Delta t}(J)\, \hat{K}_J^{\varphi\dagger} \partial_\varphi \hat{K}_J^{\varphi}\Big|_{\varphi=0} \\
&= \Delta t \begin{bmatrix} -\frac{1}{2}\partial_\varphi(\hat{L}_\varphi^\dagger \hat{L}_\varphi) \\ +\hat{L}_\varphi^\dagger \partial_\varphi \hat{L}_\varphi \end{bmatrix}\Bigg|_{\varphi=0} + \mathcal{O}(\Delta t^2) \\
&= \frac{\Gamma \Delta t}{2}\left(\hat{J}_z \hat{J}_- - \hat{J}_+ \hat{J}_z\right) + \mathcal{O}(\Delta t^2). \qquad \text{(K32)}
\end{aligned}$$

The term $\hat{L}_\varphi^\dagger \partial_\varphi \hat{L}_\varphi \Delta t$ originates from the product of the two terms proportional to $J\Delta t$ in $\hat{K}_J^{\varphi\dagger}$ and $\partial_\varphi \hat{K}_J^{\varphi}$. At $\varphi = 0$ and $\theta = 0$, the initial Dicke state and all preceding Kraus operators are real in the Dicke basis, whereas the order-Δt part of the operator above is real and antisymmetric. Consequently, for every measurement record, its expectation value immediately before the current measurement step vanishes. Integrating the later outcomes leaves a contribution of order $\mathcal{O}(\Delta t^2)$ from each time step; summing over $M = t/\Delta t$ steps gives $\mathcal{O}(t\Delta t)$, which vanishes in the continuous-time limit. Hence, $\langle \Psi_\varphi(t)|\partial_\varphi \Psi_\varphi(t)\rangle|_{\varphi=0} \to 0$ as $\Delta t \to 0$. We conclude that, as in photon counting, the joint quantum Fisher information, in terms of the Kraus operators, can be expressed as

$$\begin{aligned}
\mathcal{F}_\varphi(|\Psi_\varphi(t)\rangle) &= 4\langle \partial_\varphi \Psi_\varphi(t)|\partial_\varphi \Psi_\varphi(t)\rangle \\
&= 4\int_{-\infty}^{+\infty} \mathrm{d}J_M\, q_{\Delta t}(J_M) \cdots \int_{-\infty}^{+\infty} \mathrm{d}J_1\, q_{\Delta t}(J_1) \\
&\quad \cdot \left\| \sum_{j=1}^{M} \hat{K}_{J_M}^{\varphi} \cdots (\partial_\varphi \hat{K}_{J_j}^{\varphi}) \cdots \hat{K}_{J_1}^{\varphi} |\psi\rangle \right\|^2 .
\end{aligned} \qquad \text{(K33)}$$

Fisher information of the continuous measurements. Let us focus on the Fisher information that can be extracted from observing the continuous-measurement trajectories. The probability of observing a certain trajectory $(i_1, i_2, \cdots, i_M)$ is

$$p_{\mathrm{traj}}(\varphi) \propto \|\hat{K}_{i_M}^{\varphi} \hat{K}_{i_{M-1}}^{\varphi} \cdots \hat{K}_{i_2}^{\varphi} \hat{K}_{i_1}^{\varphi} |\psi\rangle\|^2. \qquad \text{(K34)}$$

Having defined the unnormalized state $|\tilde{\psi}_{\mathrm{traj}}(\varphi)\rangle$ associated with a certain observed trajectory in Eq. (K17), we can write $p_{\mathrm{traj}}(\varphi) \propto \langle \tilde{\psi}_{\mathrm{traj}}(\varphi)|\tilde{\psi}_{\mathrm{traj}}(\varphi)\rangle$, where we have omitted the dependence on the time t. The definition of the Fisher information obtainable from the trajectories is

$$F^{c,h} \equiv \mathbb{E}_{\mathrm{traj}}\left[\left(\frac{\partial \log p_{\mathrm{traj}}(\varphi)}{\partial \varphi}\right)^2\right]. \qquad \text{(K35)}$$

We can evaluate the derivative of $\log p_{\mathrm{traj}}(\varphi)$ as follows:

$$\begin{aligned}
\frac{\partial \log p_{\mathrm{traj}}(\varphi)}{\partial \varphi} &= \frac{1}{\langle \tilde{\psi}_{\mathrm{traj}}(\varphi)|\tilde{\psi}_{\mathrm{traj}}(\varphi)\rangle}\Big(\langle \partial_\varphi \tilde{\psi}_{\mathrm{traj}}(\varphi)|\tilde{\psi}_{\mathrm{traj}}(\varphi)\rangle \\
&\quad + \langle \tilde{\psi}_{\mathrm{traj}}(\varphi)|\partial_\varphi \tilde{\psi}_{\mathrm{traj}}(\varphi)\rangle\Big). \qquad \text{(K36)}
\end{aligned}$$

We define $|\partial_\varphi \tilde{\psi}_{\mathrm{traj}}(\varphi)\rangle \equiv \sqrt{p_{\mathrm{traj}}(\varphi)}|\phi_{\mathrm{traj}}(\varphi)\rangle$ and write the classical Fisher information as

$$\begin{aligned}
F^{c,h} &= \sum_{\mathrm{traj}} p_{\mathrm{traj}}(\varphi)(\langle \psi_{\mathrm{traj}}(\varphi)|\phi_{\mathrm{traj}}(\varphi)\rangle \\
&\quad + \langle \phi_{\mathrm{traj}}(\varphi)|\psi_{\mathrm{traj}}(\varphi)\rangle)^2. \qquad \text{(K37)}
\end{aligned}$$

Following [34], we define $A_{\mathrm{traj}} \equiv \langle \phi_{\mathrm{traj}}(\varphi)|\psi_{\mathrm{traj}}(\varphi)\rangle$, and we write the Fisher information in Eq. (K37) under the assumption $A_{\mathrm{traj}} \in \mathbb{R}$, which we will prove to be satisfied in the scenario we consider for photon counting and homodyne detection. With this simplification, we can write Eq. (K37) as

$$F^{c,h} = 4\sum_{\mathrm{traj}} p_{\mathrm{traj}}(\varphi) A_{\mathrm{traj}}^2. \qquad \text{(K38)}$$

Fisher information of the spins. From Eq. (K9), we see that in order to complete the assessment of how much information is retrievable through continuous measurements, we need to compute the quantum Fisher information for the last measurement on the spin ensemble in addition to the Fisher information from the continuous measurements. Although we will always be interested in the asymptotic case where the final state of the ensemble is independent of the trajectory, in this paragraph we work at a generic time t. Consider the expectation value of the Fisher information of the spins over the trajectory,

$$\begin{aligned}
\mathbb{E}_{\mathrm{traj}}[\mathcal{F}_\varphi(|\psi_{\mathrm{traj}}(\varphi)\rangle)] &= 4\sum_{\mathrm{traj}} p_{\mathrm{traj}}(\varphi) \\
&\quad \cdot (\langle \partial_\varphi \psi_{\mathrm{traj}}(\varphi)|\partial_\varphi \psi_{\mathrm{traj}}(\varphi)\rangle + (\langle \partial_\varphi \psi_{\mathrm{traj}}(\varphi)|\psi_{\mathrm{traj}}(\varphi)\rangle)^2).
\end{aligned} \qquad \text{(K39)}$$

Introducing again the states $|\phi_{\mathrm{traj}}(\varphi)\rangle$, we can obtain an alternative expression for the QFI through the use of the identity

$$|\partial_\varphi \psi_{\mathrm{traj}}(\varphi)\rangle \equiv |\phi_{\mathrm{traj}}(\varphi)\rangle - A_{\mathrm{traj}}|\psi_{\mathrm{traj}}(\varphi)\rangle, \qquad \text{(K40)}$$

and, assuming A_{traj} is real, we see that we can rewrite the quantum Fisher information of the system of spins as

$$\mathcal{F}_\varphi(|\psi_{\mathrm{traj}}(\varphi)\rangle) = 4(\langle \phi_{\mathrm{traj}}(\varphi)|\phi_{\mathrm{traj}}(\varphi)\rangle - A_{\mathrm{traj}}^2), \qquad \text{(K41)}$$

as already shown in Ref. [34]. Since we are in the regime of single-parameter estimation, this QFI is achievable

through the optimal measurement on the spin ensemble. Combining the Fisher information of the continuous measurement with that of the spin-ensemble measurement (averaged over trajectories), we get the following expression

$$F^{h,c} \equiv F^{h,c}(p_{\text{traj}}) + \mathbb{E}_{\text{traj}}[\mathcal{F}_\varphi(|\psi_{\text{traj}}(\varphi)\rangle)] = 4\sum_{\text{traj}} \langle\tilde{\psi}_{\text{traj}}(\varphi)|\tilde{\psi}_{\text{traj}}(\varphi)\rangle\langle\phi_{\text{traj}}(\varphi)|\phi_{\text{traj}}(\varphi)\rangle. \quad \text{(K42)}$$

Fisher information of photon counting. Writing explicitly the expression for $|\phi_{\text{traj}}(\varphi)\rangle$, we easily see that Eq. (K42) is identical to Eq. (K28). It remains to prove that A_{traj} is real. This is easily done by considering the explicit expression for the unnormalized evolved state in the Dicke basis. The initial state $|m_0\rangle$, expressed in this basis, has only real components. The operators $\hat{K}_0^\varphi$ and $\hat{K}_1^\varphi$ in Eq. (K14), expressed in the Dicke basis, are real matrices for $\varphi = 0$, so that the state $|\psi_{\text{traj}}(\varphi = 0)\rangle$ is also real. Consider now the derivatives of the Kraus operators, which are necessary to compute $|\phi_{\text{traj}}(\varphi)\rangle$:

$$\frac{\partial \hat{K}_0^\varphi}{\partial\varphi} = -\frac{1}{2}\Delta t \frac{\partial(\hat{L}_\varphi^\dagger \hat{L}_\varphi)}{\partial\varphi}\hat{K}_0^\varphi + \mathcal{O}(\Delta t^2) = \frac{1}{2}\Gamma\Delta t(\{\hat{J}_x, \hat{J}_z\} - \hat{J}_x) + \mathcal{O}(\Delta t^2), \quad \text{(K43)}$$

and

$$\frac{\partial \hat{K}_1^\varphi}{\partial\varphi} = \sqrt{\Delta t}\frac{\partial \hat{L}_\varphi}{\partial\varphi} = -\sqrt{\Delta t\Gamma}\hat{J}_z. \quad \text{(K44)}$$

Both these operators, when expressed as matrices in the canonical Dicke basis, have real entries. Therefore, we conclude that $A_{\text{traj}} \equiv \langle\phi_{\text{traj}}(\varphi)|\psi_{\text{traj}}(\varphi)\rangle \in \mathbb{R}$, and that the Fisher information computed from the trajectories of the photon-counting measurements achieves the quantum Fisher information.

Fisher information of homodyne detection. We now repeat the same argument for homodyne detection. Starting from Eq. (K15), we see that, with $\hat{H} = 0$, the operator $\hat{K}_J$ is real if we assume $\theta = 0$. When taking the derivative, we have that both $\frac{\partial(\hat{L}_\varphi^\dagger \hat{L}_\varphi)}{\partial\varphi}$ and $\frac{\partial \hat{L}_\varphi}{\partial\varphi}$ are real, as proved in the previous paragraph. Therefore, the condition $A_{\text{traj}} \in \mathbb{R}$ also holds for homodyne detection, and this measurement saturates the QFI.

Limitations of the proof. This proof, based on the fact that A_{traj} has no imaginary part, fails when $\hat{H} \neq 0$ (which happens when the cavity is detuned) or when the generator of the rotation has imaginary components, as happens for the twist-untwist encoding in Eq. (6), which uses squeezing in the initial state of the ensemble. This does not necessarily mean that homodyne detection and photon counting cannot achieve the QFI in this case, but it means that the achievability of the QFI through continuous measurement cannot be proven within the framework developed in this appendix.

APPENDIX L: CONTINUOUS ENCODING

In this appendix, we extend the formalism of matched filtering to continuous encoding. We again assess the capabilities of the homodyne and photon counting measurements. We consider sensing the parameter φ encoded by the Hamiltonian term $\varphi\hat{G}$ acting continuously on the spin ensemble. We denote by $\mathcal{L}$ the Lindbladian operator describing the superradiant decay of the spin ensemble, so that by adding the continuous encoding we can write $\mathcal{L}_\varphi \equiv \mathcal{L} - i\varphi[\hat{G}, \cdot]$. The corresponding Heisenberg-picture generator is $\mathcal{L}_\varphi^\dagger \equiv \mathcal{L}^\dagger + i\varphi[\hat{G}, \cdot]$. We consider the Heisenberg-evolved jump operator $\hat{J}_-^\varphi(t)$, and we are interested in evaluating its parametric derivative to plug it into Eq. (9), in order to obtain the output-field signal. To achieve this, the parametric derivative of the evolution operator is useful and can be computed from the following integral:

$$\frac{\partial}{\partial\varphi} e^{\mathcal{L}_\varphi^\dagger t}\bigg|_{\varphi=0} = t\int_0^1 ds\, e^{(1-s)\mathcal{L}^\dagger t}\frac{\partial \mathcal{L}_\varphi^\dagger}{\partial\varphi} e^{s\mathcal{L}^\dagger t}. \quad \text{(L1)}$$

The parametric derivative of the Heisenberg-picture generator is the commutator, i.e., $\frac{\partial \mathcal{L}_\varphi^\dagger}{\partial\varphi} = +i[\hat{G}, \cdot]$. Applying this formula to the jump operator gives the final formula for the derivative of the lowering operator $\hat{J}_-^\varphi(t)$:

$$\frac{\partial \hat{J}_-^\varphi(t)}{\partial\varphi}\bigg|_{\varphi=0} = +it\int_0^1 ds\, e^{(1-s)\mathcal{L}^\dagger t}([\hat{G}, e^{s\mathcal{L}^\dagger t}(\hat{J}_-)]). \quad \text{(L2)}$$

From the above expression we can evaluate the output-field signal

$$\alpha_I(t) = -i\sqrt{\Gamma}\left\langle \frac{\partial \hat{J}_-^\varphi(t)}{\partial\varphi}\bigg|_{\varphi=0}\right\rangle = t\sqrt{\Gamma}\int_0^1 ds\left\langle e^{(1-s)\mathcal{L}^\dagger t}([\hat{G}, e^{s\mathcal{L}^\dagger t}(\hat{J}_-)])\right\rangle. \quad \text{(L3)}$$

The corresponding homodyne-current response is $2\text{Re}[e^{i\theta}\alpha_I(t)]$, consistent with the definition in Eq. (12).

The correlation function of the outcomes is still given by Eq. (24), since the infinitesimally small perturbation caused by φ does not change the state of the system to zeroth order in φ. The result for the mode maximizing the SNR in Eq. (26) is still valid for continuous encoding. In the photon counting scenario, we can derive a similar expression by computing the parametric derivative of the correlation function $g_1(t', t; \varphi)$.

[1] R. H. Dicke, *Coherence in spontaneous radiation processes*, Phys. Rev. **93**, 99 (1954).

[2] M. Gross and S. Haroche, *Superradiance: An essay on the theory of collective spontaneous emission*, Phys. Rep. **93**, 301 (1982).

[3] N. E. Rehler and J. H. Eberly, *Superradiance*, Phys. Rev. A **3**, 1735 (1971).

[4] A. Asenjo-Garcia, M. Moreno-Cardoner, A. Albrecht, H. Kimble, and D. Chang, *Exponential improvement in photon storage fidelities using subradiance and "selective radiance" in atomic arrays*, Phys. Rev. X **7**, 031024 (2017).

[5] F. Mivehvar, H. Ritsch, and F. Piazza, *Superradiant topological peierls insulator inside an optical cavity*, Phys. Rev. Lett. **118**, 073602 (2017).

[6] S. J. Masson and A. Asenjo-Garcia, *Universality of Dicke superradiance in arrays of quantum emitters*, Nat. Commun. **13**, 2285 (2022).

[7] D. Malz, R. Trivedi, and J. I. Cirac, *Large-N limit of Dicke superradiance*, Phys. Rev. A **106**, 013716 (2022).

[8] O. Rubies-Bigorda, S. Ostermann, and S. F. Yelin, *Characterizing superradiant dynamics in atomic arrays via a cumulant expansion approach*, Phys. Rev. Res. **5**, 013091 (2023).

[9] B. Sundar, D. Barberena, A. M. Rey, and A. P. n. Orioli, *Squeezing multilevel atoms in dark states via cavity superradiance*, Phys. Rev. Lett. **132**, 033601 (2024).

[10] X. H. H. Zhang, D. Malz, and P. Rabl, *Unraveling superradiance: Entanglement and mutual information in collective decay*, Phys. Rev. Lett. **135**, 033602 (2025).

[11] J. G. Bohnet, Z. Chen, J. M. Weiner, D. Meiser, M. J. Holland, and J. K. Thompson, *A steady-state superradiant laser with less than one intracavity photon*, Nature (London) **484**, 78 (2012).

[12] Z. Yan, J. Ho, Y.-H. Lu, S. J. Masson, A. Asenjo-Garcia, and D. M. Stamper-Kurn, *Superradiant and subradiant cavity scattering by atom arrays*, Phys. Rev. Lett. **131**, 253603 (2023).

[13] S. L. Kristensen, E. Bohr, J. Robinson-Tait, T. Zelevinsky, J. W. Thomsen, and J. H. Müller, *Subnatural linewidth superradiant lasing with cold 88Sr atoms*, Phys. Rev. Lett. **130**, 223402 (2023).

[14] C. Liedl, F. Tebbenjohanns, C. Bach, S. Pucher, A. Rauschenbeutel, and P. Schneeweiss, *Observation of superradiant bursts in a cascaded quantum system*, Phys. Rev. X **14**, 011020 (2024).

[15] E. Y. Song, D. Barberena, D. J. Young, E. Chaparro, A. Chu, S. Agarwal, Z. Niu, J. T. Young, A. M. Rey, and J. K. Thompson, *A dissipation-induced superradiant transition in a strontium cavity-QED system*, Sci. Adv. **11**, eadu5799 (2025).

[16] W. Kersten, N. de Zordo, O. Diekmann, E. S. Redchenko, A. N. Kanagin, A. Angerer, W. J. Munro, K. Nemoto, I. E. Mazets, S. Rotter, T. Pohl, and J. Schmiedmayer, *Self-induced superradiant masing*, Nat. Phys. **22**, 158 (2026).

[17] F. E. van Dorsselaer and G. Nienhuis, *Collective decay as a stochastic process*, Phys. Rev. A **56**, 958 (1997).

[18] M. Perarnau-Llobet, A. González-Tudela, and J. I. Cirac, *Multimode Fock states with large photon number: Effective descriptions and applications in quantum metrology*, Quantum Sci. Technol. **5**, 025003 (2020).

[19] B. Lemberger and K. Mølmer, *Radiation eigenmodes of Dicke superradiance*, Phys. Rev. A **103**, 033713 (2021).

[20] A. González-Tudela, V. Paulisch, D. E. Chang, H. J. Kimble, and J. I. Cirac, *Deterministic generation of arbitrary photonic states assisted by dissipation*, Phys. Rev. Lett. **115**, 163603 (2015).

[21] V. Paulisch, M. Perarnau-Llobet, A. González-Tudela, and J. I. Cirac, *Quantum metrology with one-dimensional superradiant photonic states*, Phys. Rev. A **99**, 043807 (2019).

[22] E. Abbasgholinejad, D. Malz, A. Asenjo-Garcia, and R. Trivedi, *Theory of quantum-enhanced interferometry with general Markovian light sources*, arXiv:2504.05111.

[23] M. Jirasek, I. Lesanovsky, and A. Cabot, *Boundary time crystal as a light source for collectively enhanced sensing*, Phys. Rev. A **114**, 032611 (2026).

[24] S. Gammelmark and K. Mølmer, *Fisher information and the quantum Cramér-Rao sensitivity limit of continuous measurements*, Phys. Rev. Lett. **112**, 170401 (2014).

[25] F. Albarelli, M. A. C. Rossi, M. G. A. Paris, and M. G. Genoni, *Ultimate limits for quantum magnetometry via time-continuous measurements*, New J. Phys. **19**, 123011 (2017).

[26] Strictly speaking, the emitted field contains exactly N photons at the reference point $\varphi = 0$; for any non-zero φ there is population for smaller numbers of photons, but we are interested in infinitesimal rotation angles and in studying the metrological properties of the N-photon state.

[27] P. M. Woodward, *Probability and Information Theory: With Applications to Radar* (McGraw-Hill, New York, 1953).

[28] G. Turin, *An introduction to matched filters*, IRE Trans. Inf. Theory **6**, 311 (1960).

[29] B. Picinbono, *Generalized matched filters*, in *Fifth ASSP Workshop on Spectrum Estimation and Modeling* (1990), pp. 182–186.

[30] V. Olshevsky and L. Sakhnovich, *Matched filtering for generalized stationary processes*, IEEE Trans. Inf. Theory **51**, 3308 (2005).

[31] E. Davis, G. Bentsen, and M. Schleier-Smith, *Approaching the Heisenberg limit without single-particle detection*, Phys. Rev. Lett. **116**, 053601 (2016).

[32] O. Hosten, R. Krishnakumar, N. J. Engelsen, and M. A. Kasevich, *Quantum phase magnification*, Science **352**, 1552 (2016).

[33] F. Albarelli and M. G. Genoni, *A pedagogical introduction to continuously monitored quantum systems and measurement-based feedback*, Phys. Lett. A **494**, 129260 (2024).

[34] R. Mattes, A. Cabot, F. Carollo, and I. Lesanovsky, *Designing open quantum systems for enabling quantum enhanced sensing through classical measurements*, Phys. Rev. Lett. **135**, 230402 (2025).

[35] A. Angerer, K. Streltsov, T. Astner, S. Putz, H. Sumiya, S. Onoda, J. Isoya, W. J. Munro, K. Nemoto, J. Schmiedmayer, and J. Majer, *Superradiant emission from colour centres in diamond*, Nat. Phys. **14**, 1168 (2018).

[36] C. Bradac, M. T. Johnsson, M. v. Breugel, B. Q. Baragiola, R. Martin, M. L. Juan, G. K. Brennen, and T. Volz, *Room-temperature spontaneous superradiance from single diamond nanocrystals*, Nat. Commun. **8**, 1205 (2017).

[37] J. J. Borkowski, A. Czerwinski, and P. Kolenderski, *Revisiting superradiance dynamics from single diamond nanocrystals with a physically consistent model for fluorescence decay*, Nat. Commun. **17**, 58 (2026).
[38] M. Mamaev, J. Venkatraman, M. Koppenhöfer, A. C. B. Jayich, and A. A. Clerk, *Detecting quantum noise of a solid-state spin ensemble with dispersive measurement*, Phys. Rev. Res. **8**, 023331 (2026).
[39] J. G. Bohnet, Z. Chen, J. M. Weiner, K. C. Cox, and J. K. Thompson, *Active and passive sensing of collective atomic coherence in a superradiant laser*, Phys. Rev. A **88**, 013826 (2013).
[40] J. M. Weiner, K. C. Cox, J. G. Bohnet, Z. Chen, and J. K. Thompson, *Superradiant Raman laser magnetometer*, Appl. Phys. Lett. **101**, 261107 (2012).
[41] A. A. Svidzinsky, L. Yuan, and M. O. Scully, *Quantum amplification by superradiant emission of radiation*, Phys. Rev. X **3**, 041001 (2013).
[42] O. Somech and E. Shahmoon, *Quantum entangled states of a classically radiating macroscopic spin*, PRX Quantum **5**, 010349 (2024).
[43] D. Meiser and M. J. Holland, *Intensity fluctuations in steady-state superradiance*, Phys. Rev. A **81**, 063827 (2010).
[44] M. Koppenhöfer, P. Groszkowski, H.-K. Lau, and A. A. Clerk, *Dissipative superradiant spin amplifier for enhanced quantum sensing*, PRX Quantum **3**, 030330 (2022).
[45] M. Koppenhöfer, P. Groszkowski, and A. A. Clerk, *Squeezed superradiance enables robust entanglement-enhanced metrology even with highly imperfect readout*, Phys. Rev. Lett. **131**, 060802 (2023).
[46] E. A. Bohr, S. L. Kristensen, C. Hotter, S. A. Schäffer, J. Robinson-Tait, J. W. Thomsen, T. Zelevinsky, H. Ritsch, and J. H. Müller, *Collectively enhanced Ramsey readout by cavity sub- to superradiant transition*, Nat. Commun. **15**, 1084 (2024).
[47] R. Bonifacio, P. Schwendimann, and F. Haake, *Quantum statistical theory of superradiance. I*, Phys. Rev. A **4**, 302 (1971).
[48] Our results should therefore be understood for a scaling of the physical parameters in N for which this condition remains satisfied as N is varied.
[49] M. A. Norcia, R. J. Lewis-Swan, J. R. K. Cline, B. Zhu, A. M. Rey, and J. K. Thompson, *Cavity-mediated collective spin-exchange interactions in a strontium superradiant laser*, Science **361**, 259 (2018).
[50] V. Giovannetti, S. Lloyd, and L. Maccone, *Advances in quantum metrology*, Nat. Photonics **5**, 222 (2011).
[51] L. Pezzè, *Quantum metrology with nonclassical states of atomic ensembles*, Rev. Mod. Phys. **90**, 035005 (2018).
[52] C. L. Degen, F. Reinhard, and P. Cappellaro, *Quantum sensing*, Rev. Mod. Phys. **89**, 035002 (2017).
[53] M. S. Scharnagl, T. Kielinski, and K. Hammerer, *Optimal Ramsey interferometry with echo protocols based on one-axis twisting*, Phys. Rev. A **108**, 062611 (2023).
[54] M. Koppenhöfer and A. A. Clerk, *Revisiting the impact of dissipation on time-reversed one-axis-twist quantum-sensing protocols*, Phys. Rev. Res. **5**, 043279 (2023).
[55] A. A. Clerk, M. H. Devoret, S. M. Girvin, F. Marquardt, and R. J. Schoelkopf, *Introduction to quantum noise, measurement, and amplification*, Rev. Mod. Phys. **82**, 1155 (2010).
[56] C. Gardiner and P. Zoller, *Quantum Noise: A Handbook of Markovian and Non-Markovian Quantum Stochastic Methods with Applications to Quantum Optics* (Springer Science & Business Media, Berlin and Heidelberg, Germany, 2004).
[57] V. V. Albert and L. Jiang, *Symmetries and conserved quantities in Lindblad master equations*, Phys. Rev. A **89**, 022118 (2014).
[58] D. F. Walls and G. J. Milburn, *Quantum Optics* (Springer Science & Business Media, Berlin and Heidelberg, Germany, 2024).
[59] C. K. Law and S. K. Y. Lee, *Dynamic photon-mode selection in Dicke superradiance*, Phys. Rev. A **75**, 033813 (2007).
[60] Note that one does not have to worry about $S_{II}(t,t')$ being non-invertible. Non-invertibility would imply the existence of one or more modes that have zero fluctuations in one quadrature. This would in turn imply infinite squeezing, something that is impossible with a finite number of photons. In our case, there is even a stronger constraint, as the superradiant decay dynamics never generates squeezing correlations in the output field.
[61] D. Yang, M. Ketkar, K. Audenaert, S. F. Huelga, and M. B. Plenio, *Quantum Cramér-Rao precision limit of noisy continuous sensing*, Phys. Rev. Lett. **136**, 070802 (2026).
[62] G. Tóth and I. Apellaniz, *Quantum metrology from a quantum information science perspective*, J. Phys. A **47**, 424006 (2014).
[63] M. Hayashi, *Asymptotic Theory of Quantum Statistical Inference: Selected Papers* (World Scientific, Singapore, 2005), 10.1142/5630.
[64] A. Khan, F. Albarelli, and A. Datta, *A tensor network approach to sensing quantum light-matter interactions*, PRX Quantum **6**, 040343 (2025).
[65] A. H. Kiilerich and K. Mølmer, *Input-output theory with quantum pulses*, Phys. Rev. Lett. **123**, 123604 (2019).
[66] A. H. Kiilerich and K. Mølmer, *Quantum interactions with pulses of radiation*, Phys. Rev. A **102**, 023717 (2020).
[67] J. Combes, K., and M. Sarovar, *The SLH framework for modeling quantum input-output networks*, Adv. Phys. **2**, 784 (2017).
[68] H. J. Carmichael, *Quantum trajectory theory for cascaded open systems*, Phys. Rev. Lett. **70**, 2273 (1993).
[69] C. Catana, L. Bouten, and M. Guta, *Fisher informations and local asymptotic normality for continuous-time quantum Markov processes*, J. Phys. A **48**, 365301 (2015) 10.1088/1751-8113/48/36/365301.
[70] D. Yang, M. Ketkar, K. Audenaert, S. F. Huelga, and M. B. Plenio, *Quantum Cramer-Rao precision limit of noisy continuous sensing*, Phys. Rev. Lett. **136**, 070802 (2025).
[71] D. Yang, S. F. Huelga, and M. B. Plenio, *Efficient information retrieval for sensing via continuous measurement*, Phys. Rev. X **13**, 031012 (2023).
[72] F. Girotti, A. Godley, and M. Guta, *Estimating quantum Markov chains using coherent absorber post-processing and pattern counting estimator*, Quantum **9**, 1835 (2025).
[73] F. Ciccarello, S. Lorenzo, V. Giovannetti, and G. M. Palma, *Quantum collision models: Open system dynamics from repeated interactions*, Phys. Rep. **954**, 1 (2022).
[74] H. M. Wiseman and G. J. Milburn, *Quantum Measurement and Control* (Cambridge University Press, Cambridge, 2009).